PERFORMANCE ASSESSMENT OF EXTERIOR BEAM COLUMN JOINT RETROFITTED USING ECC

A dissertation submitted in the partial fulfillment of the requirements for the award of the degree of

MASTER OF ENGINEERING
IN
STRUCTURAL ENGINEERING

BY

Navin Devkota

801724017

UNDER THE SUPERVISION OF

Dr. Prem Pal Bansal
Associate Professor & Head
Department of Civil Engineering

Mr. Raju Sharma
Lecturer
Department of Civil Engineering

CIVIL ENGINEERING DEPARTMENT

THAPAR INSTITUTE OF ENGINEERING & TECHNOLOGY
(A DEEMED TO BE UNIVERSITY)
PATIALA, PUNJAB

JULY, 2019

DECLARATION

I, **Navin Devkota**, hereby declare that the work presented in this thesis entitled **"PERFORMANCE ASSESSMENT OF EXTERIOR BEAM COLUMN JOINT RETROFITTED USING ECC"** in fulfillment of the requirement for the award of degree of **Master of Engineering** in **Structural Engineering** submitted at **Civil Engineering Department, Thapar Institute of Engineering & Technology, Patiala**, is an authentic record of work carried out under the guidance of **Dr. Prem Pal Bansal, Associate Professor & Head of Department and Mr. Raju Sharma, Lecturer, Thapar Institute of Engineering & Technology, Patiala.** The matter presented in this has not been submitted either in part or full to any other university or institute for the award of any other degree.

Navin Devkota

(801724017)

Date: 30 July 2019

This is to certify that the above declaration made by the student concerned is correct according to the best of my knowledge and belief.

Dr Prem Pal Bansal
Associate Professor & Head
Department of Civil Engineering
Thapar Institute of Engineering and Technology

Mr. Raju Sharma
Lecturer
Department of Civil Engineering
Thapar Institute of Engineering and Technology

i

ACKNOWLEDGMENT

I would like to express my heart full appreciations to all the associated persons who directly and indirectly support me to accomplish this thesis get done. It would not be fair on my part if I don't say a word of thanks to all those whose sincere advice made this period an educative, enlightening, pleasurable and memorable one.

Primarily, I would like to express my special thanks of gratitude to **Dr. Prem Pal Bansal Associate Professor & Head Of Department**, Department of Civil Engineering, Thapar Institute of Engineering and Technology, Patiala, for providing his valuable guidance and support that helped me patch this project report and make it a full proof success. His suggestions and instructions have served as the major contributor to the completion of the dissertation.

I would like to extend my deep gratitude to **Mr. Raju Sharma, Lecturer** Department of Civil Engineering, Thapar Institute of Engineering and Technology, Patiala, for his valuable guidance and motivation bestowed upon me for successful completion of the dissertation and I will fell gratitude for it. It could not be possible to accomplish this pursuit without his mentorship. His timely advice, meticulous scrutiny and scholarly advice have helped me to a great extent to accomplish this task.

Last but not least, I would like to thank Mr. Virendar Sharma, Mr. Manpreet Sing and Mr. Hitesh Bharadwja and Mr. Ramsimran for regular cooperation and help during the period of work.

Navin Devkota
801724017

ABSTRACT

The structural integrity is significantly depends on the behavior of beam-column joint during earthquake. The earthquake occurred in Nepal, India, Pakistan and Japan have been facing disastrous consciences attributed to failure of beam column joint. Adopted design philosophy in these countries lacks the ductile detailing in the past design which led to extensive cracks in beam column joint zone and failure occurs. This attracts the need on the research and development of repaid repairing techniques of damaged structural element. The confinement has been considered rapid repairing technique proven to be efficient in restoring original capacity. However, Engineered cementitious concrete (ECC) are the new composite techniques formulated using micro mechanics and exhibit straining hardening property, where previous composites such as FRP, steel fibers reinforced composites are limited to high compressive strength and strain softening tensile strain property.

In the present dissertation, the effort has been made to implement the ECC as a retrofitting material to strengthen the initially distress beam column joint. Therefore, initially, the ECC has been developed to attain the higher tensile strain. Further, the beam column joint is damaged to obtain the complete and moderate initial damage levels which are calculated using Park and Ang damage indices model. The retrofitted specimens were subjected to quasi static cyclic loading (QSCL) under controlled deformation until failure. The initially damaged specimen has been retrofitted using ECC. The load-deflection relationship, ductility, stiffness and strength degradation, energy dissipation capacity and joint shear stress of controlled and ECC retrofitted specimens have been compared. The test results indicated that the use of ECC materials in the joint zone as a retrofitting material can enhance the joint shear stress capacity, stiffness and strength degradation, as well as the energy dissipation as compared to controlled specimens. However the performance of retrofitted specimen significantly depends upon the initial damage level of the beam column joint.

TABLE OF CONTENT

LIST OF TABLES

LIST OF FIGURE

CHAPTER 1

INTRODUCTION

1.1 GENERAL

The numbers of life threatening catastrophic structure failures have been experienced due to past earthquake such as Kangara earthquake 1905, Nepal–Bihar earthquake 1934, Turkey and Taiwan in 1999. It takes more than 30000 lives of innocent human beings. It is not the earthquake takes life of people; it's due to the failure of man-made structure during earthquake. Most of the failure attributes caused by downfall of beam-column joint at the time of earthquake due to brittle failure of beam-column joint. Figure1.1 shows deadly earthquake consequence in Turkey in 1999. Generally in moment resisting RCC structure, three different types joints are designed especially for particular location of the grid-interior joint, exterior joint and corner joint shown in Figure 1.2.

Figure 1.1 Exterior beam column joint failure in earthquake in Turky1999 *(www.britannica.com)*

1.2 TYPES OF BEAM COLUMN JOINTS

The joint section in RCC frame is termed as the common section of the column and beam where within the column the depth of the beam frames inside the column (ACI 352-02). In general, there are two types of joints (type I and II) based on the concrete frame type. If the concrete frame is designed to carry gravity loads and no inelastic deformations are required, then the joints are called type I. If the concrete frame is designed to carry the gravity loads and resist lateral loads inelastic deformations is required to dissipate energy, and then the joints are called

type II. The earlier codes required the framing members of the joint to be designed according to their prevailing stresses, but the design of the joints was ignored in these codes. Most of the buildings were destroyed during earthquakes caused by deficiency of the shear reinforcement in the joint regions. All type I joints have no reinforcement to resist the shear force through the joints that are characterized by:

1. Lack of transvers of reinforcement in joint region.
2. Weak column-strong beam condition
3. Weak concrete.

Type 2 joints that are constructed in reliance with modern codes characterized by:

1. Adequate transverse reinforcement ties with in the joint as shear reinforcement.
2. Adequate ductility in the joint regions
3. Strong column-weak beam joints.

All these features will prevent or delay the failure in joint and provide opportunity for the plastic hinge to form in the flexural member(s).

The beam-column joints could also be classified based on the joint position as internal and external joints or joint shape within the concrete frame. Figure 1.2 shows mainly three types of beam-column joints depend on the shape and position.

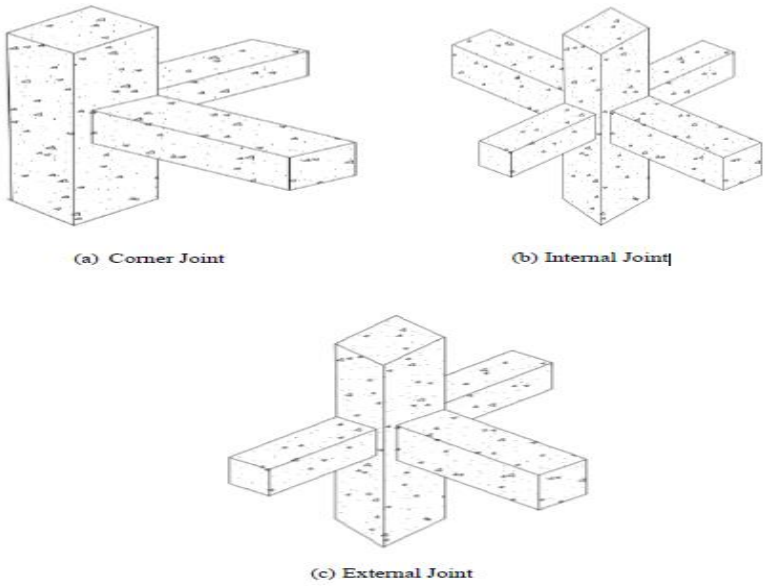

Figure 1.2 Different Types of Joint (ACI-ASCE)

1.3 MECHANISM OF BEAM COLUMN JOINT FAILURE

Joint failure occurs due to large shear input from the beam, bond deterioration of beam bars by cyclic loading and lack of confinement for joint core concrete. Earthquake resistance design philosophy gives emphasis on providing enough ductility to the frame structures so that structural member able to dissipate seismic energy without getting major cracks. Fundamentally, member ductility contributes overall structure to become ductile; ductility is achieved in the form of inelastic rotation of the joint. In reinforced concrete structural element, there is region called plastic hinge up to where inelastic rotations spread over. When inelastic deformations takes place during earthquake the original material properties crosses the elastic yield range and damages in the form of cracks start to visible in this joint periphery. Therefore, in seismic design, the damages in the plastic hinges are not accepted to be occurred in the column instead of beam.

The notion of "strong-column-weak beam" is implemented in seismic resistance design to assign beam yield. Through adequate and appropriate beam detailing, the imposed inelastic rotational demand can be achieved well. By comparison, if plastic hinge is set free to form in a vertical member, the imposed inelastic rotational requirements are very large, which makes it very hard to provide the detailing method accessible. Column yielding or story mechanism is called the mechanism with such a function. The adequate flexural strength should be provided in the column above and below the joint when the adjacent beams at their plastic hinges develop flexural over strength. The ratio of flexural column strength to flexural beam strength is a very significant parameter for beam hinge formation and ensures a powerful column relationship and weak beam relationship. Below equations conforms the moment power proportions of the column to the beam to guarantee powerful column and weak beam relationships.

Indian Standard (IS 13920 - 2014)

$$\sum M_{nc} \geq 1.4 \sum M_{nb} \tag{1}$$

As per European Code (EN1998-1:2003)

$$\sum M_{nc} \geq 1.3 \sum M_{nb} \tag{2}$$

As per New Zealand standard (NZS3101:1995)

$$\sum M_{nc} \geq 1.4 \emptyset_0 \sum M_{nb} \tag{3}$$

As per American standard (ACI 318M-02)

$$\sum M_{nc} \geq 1.2 \sum M_{nb} \quad (4)$$

Here $\emptyset_0$ is over strength of beam. M_{nc} is the total moment capacity of column and M_{nb} is the total moment capacity of beam.

1.3.1 Forces Acting on Beam Column Joint

To resist the induced shear cracks, shear reinforcement is provided. Joint efficiency has been observed to be directly influenced by the pattern of longitudinal reinforcement detailing. Figures 1.3b and 1.3c idealized some detailed patterns for the column joint of exterior beams. Figure 1.3b yields in efficiencies of 25-40 % when bars bent far reaching to the joint, while 85-100% efficiency is achieved in that anchorage area. However, the stirrups have to be provided within the joint in order to confine the concrete core. During earthquake shaking, the beams joint areas are subjected to moment's clockwise or anticlockwise direction. Under these moments, Top and bottom reinforcement bars of the joint are pulled in two different directions. The bonding stress between steel and concrete helps to balance the strength created in the joint. To maintain tight grip between steel and concrete size of the column should be large and the grade of concrete in joint region have to higher. If these conditions are not full fill the bar get slips out inside the joint region, and beams fails to carry the load. Further, top and bottom ends experienced the pull and push force during earthquake, distortion in the joint take place; one diagonal length of the joint expands and the other get compressed.

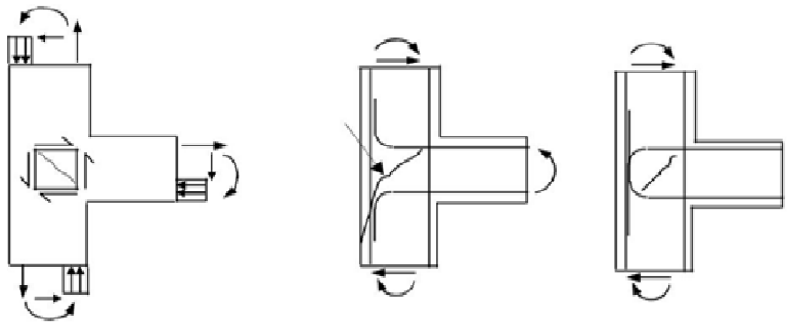

(a) (b) (c)

Figure 1.3 Responses Before and After Detailing in The Joints. (S.R. and Prasad, 2003)
(a)Forces Acting in Joint (b) Weak Detailing in Joint (c) Good Detailing

1.4 RETROFITTING

When joint experienced earthquake load, the prime reason of joint failure is gradual degradation of bond in the reinforcement and concrete matrix and result in spalling of concrete. The cyclic load promotes cracks in structure then overall integrity and stability of a concrete structure remained less than original. Because of limited time and constraint economic condition, the option of retrofitting the damaged part is the most favorable. The modification of existing structures in terms of strength and durability is termed as "retrofitting" to make more resistant toward earthquake, ground motion, or soil failure due to earthquakes.

Different methods have been practicing since long. Concrete jacketing, steel fiber jacketing, Ferro cement laminate jacketing and fibre-reinforced polymer (FRP) are most common techniques for retrofitting the beam column joints and important structural elements. Other cementitious materials including ultrahigh performance fiber reinforced concrete (UHPFRC) also used as retrofitting materials. Among all common retrofit solution, externally bonded FRP is frequently used as FRP shear retrofit of RC structures because of its many advantages such as less weight and hectic free installation, large strength to weight ratio, maximum stiffness to weight ratio. However, retrofitting by using of FRP has also limited in tensile strain capacity and vulnerable to undesirable brittle failures (Wu et al., 2014).

1.5 ENGINEERED CEMENTITIOUS COMPOSITE (ECC)

At the University of Michigan, ECC has been established with a reasonable tensile strength of 4-6MPa and a ductility of 3-5% (Li, 1993 ; Fischer et al., 2003). Engineered cement composite (ECC) is a family member of HP-FRCC and offers characteristics of various cracking conduct and tensile strain ability of over 3–7 percent with tensile strength of about 4–6 MPa with fiber content of less than 2 percent. To achieve ultra-high ductility in ECC, the composite microstructure using micromechanical models accounts for the interaction between fibres, interfaces and mortars. These methods assist with only the mild quantity of fibers to tailor these three stages synergistically. Mixing with good silica sand and admixtures such as fly ash and super plasticizers due to the elimination of coarse aggregates, ECC has high workability homogeneity. Most of the polymeric fibers are used to obtain the above-mentioned characteristics with the suitable quantity of high aspect ratio fibers and high PVA fibers tensile ability. Major polymeric fibers such as polyvinyl alcohol (PVA), polyethylene (PE) and polypropylene (PP) fibers are commonly used in ECC fibers development. New type of

cemented composite strengthened by fiber, known as Engineered Cementitious Composite (ECC) was created. Its attributing characteristics are 3-7 percent strain hardening conduct in post yield and strain ability compared to 1.5 percent of HPFRC, although fiber content is less than or equal to 2 percent. With a diameter of less than 50 microns, the micromechanical calculation favors strain hardening with reduced fiber volume fraction. Consequently, polymeric fibers preferred steel fibers, typically between 150 and 500 microns.

1.5.1 Historical Development

The evolution of fiber reinforced concrete takes numbers of phases. Romauldi and Mandel, (1964) demonstrated concrete incorporating steel fiber aiming of reducing brittle nature of concrete. The experiments are continued with different range of fibers, for instance carbon, synthetic, natural fibers and currently hybrid that contains different fibers and varying length. This knowledge is resulted in structure design recommended by RILEM TC 162-TDF. This document is solely for fiber reinforced concrete possesses tensile softening quasi-brittle response.The beginning of 1980's enthusiasm of creating fiber reinforced concrete shows ductility in tension has been gaining ground. The fiber reinforced cement succeeds to achieve toughness but not ductility. Ductility is the measurement of the tensile deformation capacity of any material. (Aveston et al., 1971; Krenchel and Stang, 1989) conducted studies using aligned fibers, discovering tensile ductility many folds higher than normal concrete. The growth of discontinuous fibers at dose (4-20%), e.g. cement laminates, and in SIFCON (Slurry Infiltrated Fiber Concrete) improved tensile strength, then ordinary concrete, showing no fragility but low ductility than constant fiber (Allen, 1971; Lankard, 1986). Engineered Cementous Composite (ECC) is not considered similar as FRC, their performance is different in some degree, and tensile ductility is one of major in all. It was regarded as strain hardening response was different in nature as compare to tensile-softening response shown by FRC. The coarse aggregates are not included in this class of matrix, regarded as fiber reinforced cement mortars. Figure 1.4 illustrates the difference between the normal concrete, FRC, and HPFRCC tested under uniaxial tension load.

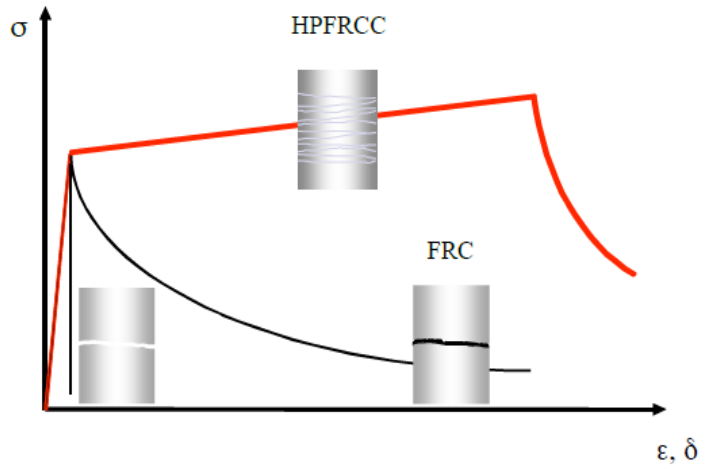

Figure 1.4 Stress Vs Deformation of Concrete, FRC and HPFRCC (Chanvillard and Rigaud, 2003**)**

In recent two class of HPFRCC have emerged. Ductal and ductility there strength are 12 MPa and 0.02-0.06 % respectively (Chanvillard and Rigaud, 2003). ECC is the result of micromechanics, synergy between fiber, matrix and interface to increase the ductility of the tensile by generating smaller multiple cracks with a total fiber volume of 2% or less by volume. Ductal performed well within elastic range only, so that fibers act effectively only on ultimate limit state (ULS) is approached, whereas ECC is intended for both elastic and inelastic area (post-yield area) where it optimally demonstrates its stress-hardening conduct.

Li, (1993) established ECC to emphasize micromechanics that in the design of ECC, prior structure does not consider the chemical and frictional bond. Micromechanics acts as a vigorous instrument to guide focused composite properties in material design and link material engineering with structural performance design. In 2006, the committee RILEM TC HFC decided to name it for this material as Strain Hardening Cementitious Composites (SHCC).. Japan Civil Engineering Society names it as "Multiple Fine Cracking Fiber Reinforced cementitious Composites". Fundamental technique behind ECC designing is follow micromechanical tolls and shown similar kind of material engineering. ECC can be considered to have tensile strengths as a family of products and these characteristics can be altered according to the requirements of a particular structure. ECC also exhibits different functionalities which of major one is high strain capacity and tiny multiple cracking. ECC (ECC M45 and its variants) is now possible to design in huge extent for onsite construction (Kong et al, 2003; Lepech and Li,

2007**).** High strength variant in early days is needed for transportation infrastructure and public traffic structures special type of ECC HES-ECC is designed for solving the particular problem in transportation infrastructure (Wang and Li, 2006). Light-weight ECC LW-ECC is designed for the normal structures bears gravity and live load only. Green ECC (G-ECC) is intended to use industrial waste products to save energy in order to decrease the carbon footprint from the building sector, supporting sustainability of facilities (Li et al., 2004; Lepech et al., 2007). Self-healing ECC (SH-ECC) focuses on transportation functionality and restoration of mechanical properties after prolonged use and damage. (Yang et al., 2005; Yang and Li, 2007). Table 1.1 demonstrates the characteristics and the unit measured for any composite structure to become ECC.

Table 1.1 Physical Attributes of ECC (Victor Li, 2002)

Compressive Strength (MPa)	First Crack Strength (MPa)	Ultimate Tensile Strength (MPa)	Ultimate Tensile Strain (%)	Young's Modulus (GPa) (MPa)	Flexural Strength (MPa)	Density (g/cc)
20-95	3-7	4-12	1-8	18-34	10-30	0.95-2.3

The most common attributes of ECC is that they have tensile ductility higher in magnitude compare to normal concrete and FRC materials.

1.5.2 ECC Material Design Principles

The ECC idea is based on fiber bridging and matrix gap expansion micro mechanics. (Li, 1993) Analysis of micromechanics described theoretically on which practical design ruled, experimental research showed that strain-hardening behavior under tensile loading can be accomplished by integrated fiber reinforcement of a cement-based matrix where the complete quantity of PVA fiber is equivalent to or less than 2% by volume. Different parts can be used in the model, but the theoretical percentage value Vf must be satisfied as given below.

$$V_f > V_f^{crit} = \frac{12J_c}{g\tau(L_f|d_f)\delta_0} \quad (5)$$

where, $\delta 0 = \tau\ Lf2\ /\ [Ef\ df\ \{1 + (Vf\ Ef)/(Vm\ Em)\}]$ represents crack opening which is directly related to the maximum bridging stress, *df* represents diameter, *Ef* is Young moduli of fiber and *Em* is Young's Moduli of matrix, snubbing factor *g*, length of fiber *Lf*, induced friction between fiber and matrix τ, *Vf* symbolize the volume factor of fiber and *Vm* represents the volume fraction of matrix. critical fiber volume fraction written as *Vcrit*, and represent matrix toughness is represent by *Jc*. Li and Leung (1992) clarified additional circumstances. Vfcrit is the critical fraction of the fiber volume and is directly dependent on the properties of fiber / matrix, matrix and fiber interaction. Fiber has its own characteristics such as length Lf, diameter df, and Ef module. The characteristics of fiber / matrix interaction include friction, and fiber / matrix property is the snubbing factor g (Li et al., 1990). The matrix modulus Em and matrix toughness Jc are the property of matrix. Fiber rupture does not allowed to take place in order satisfies above application, fiber/matrix interface is easily governed just be simple but induced friction does not contain chemical bond. Extension of equation to composite with above properties has been considered by (Kanda and Li, 1997). The new formation of formula of equation guided to *Vfcrit* which mostly relies on chemical bond strength, fiber strength and, necessary formulation and terms describes all above.

1.5.3 Constituents of ECC

ECC OPC, sand, fly ash, silica fumes, GGBS, polyvinyl alcohol fibers (PVA) and metal fibers, water and super plasticizers. Water / binder ratios usually differ between 0.3-0.56 and super plasticizers with cross ponding.

1.6 ADVANTAGE OF ECC

As compare to ordinary concrete material ECC out perform in every mechanical aspect of strength, workability and durability. Main notable advantage of ECC is its tensile strain capacity is multiple times than normal concrete. Therefore tiny multiple micro cracks less than 100 microns are formed, results of this durability against chemical and adverse environment remains longer.

Larger tensile ductility of ECC permits structural element to deform compatibly and produce synergistic loading distributing capability with steel reinforcement. As a results in better utilization of steel reinforcement and enhance structural performance.

1. ECC's tight crack nature protects steel from corrosive processes, leading in improved structural durability
2. Low fiber volume content makes less cost for ECC small fiber content is applied but do not compromise in compressive strength and ductility.
3. Primary difference in the properties between ECC and FRC is that when the ECC gets cracks in post peak load it has tendency to stain solidified whereas the FRC does not exhibits similar tendency.
4. The ECC composites has ample fracture toughness capacity can compare with aluminum alloys, and tolerance capacity of damage also high.
5. Overall cost of service life of structure is reduced; however initial cost of ECC is twice the normal concrete.
6. Shear element are best suited to retrofit using ECC since its tensile ductile performance comes in action in cyclic load.
7. Found excellent seismic resistance response and comparative very less post-earthquake repair requirement when ECC is used in place of normal concrete and reinforcement.

1.7 LIMITATION OF ECC

ECC is a modern example of concrete composite with robust strength in tensile and strain hardening property. However it has some limitation some of them are listed below given below.

1. Still in present scenario, there is limited use of ECC in structures: Expensive cost of Materials due to costlier constituents (fibers, cement and admixtures).
2. High sensitivity of the material to mixing and mix proportions.
3. It is the latest engineered material, its practice is very uncommon and limited structural have been built using ECC. Designers need the necessary knowledge to implement in field application.
4. Limited number of design code is available to design the materials.

1.8 APPLICATION OF ECC

To make ECC broadly available. Japan Society of Civil Engineers published a guide line for industrial application of ECC (JSCE 2007 ; Rokugo et all 2007).

1. Most admirable properties of energy dissipation helps in seismic resistance of multistory building.
2. It can be used as link slab of bridge decks (Kim et al, 2004; Lepech and Li, 2005). In the American continent and some part of Europe has practicing successfully .
3. ECC is successfully used as composite material decking of bridge in Japan
4. In Korea ECC is used to re strengthening the tunnel. (Wonha, 2004).
5. It can be used as repair material of dam such as, Miraka dam in Japan (Kojima et al, 2004) and Repairing work of irrigation channel in Japan (Kunieda and Rokugo, 2006)

   Housing and Industries are employing ECC in their planning stages.

Indeed, ECC offers huge space in structural innovation which was not possible in previous, since it has high ductile property which far outperformed traditional brittle concrete.

1.9 ORGANIZATION OF THESIS

This dissertation includes the following chapters:

Chapter One: Introduction presents the description of general introduction, history, constituents, design principle, advantage, limitation and application of ECC.

Chapter Two: Literature review presents a brief review of the existing literature in the area of development of ECC and retrofitting of beam column joint using ECC.

Chapter Three: Development of ECC comprises the experimental study of the materials used in the development of ECC as per IS standard and evaluate the mechanical properties of the developed ECC as per IS and ASTM standard.

Chapter Four: Experimental program gives the description of the materials used in the T beam experimentally. Furthermore, it discusses about the testing arrangement of T beams in different damage level index and examines the retrofitting strategy of the damaged beam column joint.

Chapter Five: Result and discussion reflects the response behaviors of the retrofitted beam column joint in cyclic loading till failure. The discussion based on the load-deflection analysis, stiffness vs strength degradation, energy dissipation, joint stress and crack pattern.

Chapter Six: Conclusion gives the specific finding of the experimental study.

CHAPTER 2
REVIEW OF LITERATURE

2.1 GENERAL

This chapter presents a review of the existing literature regarding the development of ECC and study the behavior of external beams-column joint of ECC composite under reversed cyclic load retrofitted using ECC.

2.2 REVIEW OF PREVIOUS LITERATURE

2.2.1 Development of ECC

This section provides a literature review concentrating on the job of numerous scientists on UHPFRC development.

Wang and Li (2007) investigated mechanical properties of ECC using large volume of fly ash and bottom ash. Focus is giving in the micro mechanics properties coordinated to composite tensile ductility on influence of large volume fly ash content. Important parameter of tensile strain capacity of composite made of sustainable material is prime concentration of this investigation. Six mixes composite were designed along with controlled ECC mix. To check compressive test 75mm diameter by 150mm height cylinder specimen used. Direct uniaxial test performed to observe tensile nature of ECC material; the coupon specimen of size (304.8 mm x 76.2 mm x 12.7 mm) used and remains left in curing tank for 28 days and tested.

OPC cement satisfies standard ASTM type 1 and fly ash contains minimum amount of calcium was tested, this fly ash were finely graded particle size distribution (average 2 micro meter) where normal class fly ash has (average 13 microns) and bottom ash (average 50 micron). Large aggregate was excluded, only fine silica sand maximum 250 micron grain size and 110 micron average grain size. PVA fibers used which have surface oil coating of 1.2 % by weight were used for all the mix composite design with no more than 2% volume fraction. Fiber consist 39 micron dia, length 12 mm and Young's modulus of 25.8 GPa. Fiber strength was 1092 MPa. Hydroxypropyl methylcellulose (HPMC), Viscosity agent and high range water reducing admixture (HRWRA) were used for good workability. Author studied the influence of high volume of fly ash along with bottom ash on the mechanical behavior of ECC. Two types of

pozzolanic materials that fly ash and bottom ash were used to replace the opc in varying amount throughout the different composite mix, but water, HRWRA and Fiber were ideal. Table 2.1 shows the mixture proportion containing fly ash and other ashes.

Table 2.1 Mixture Proportions Containing Fly Ash and Other Ashes (Wang and Li, 2007)

Mixture Id	Cement Kg/m^3	Sand Kg/m^3	Ash Kg/m^3	Water Kg/m^3	HPMC Kg/m^3	HRWRA Kg/m^3	Fiber Kg/m^3
ECC R0	838	838	-	366	1.26	17	26
ECCG0	583	467	700 (BA)	289	-	19	26
ECCG1	318	701	509(FA) 191(FFA)	289	0.16	19	26
ECCG2	318	701	701 (FA)	289	0.16	19	26
ECCG3	318	701	191(FFA) 250(FA) 250(BA	289	0.16	19	26
ECCG4	318	701	701(BA)	289	0.16	19	26

FA= Fly ash , FFA= Fine fly ash, BA= Bottom Ash

The Figure 2.1, shows the tensile stress against strain capacity of these six mixtures along with the controlled reference ECC R0 contain no fly ash. And tensile properties are also summarizing in Table 2.2. Considerable strain hardening and multiple tight cracks were observed in ECC mixtures with high volume fly ash, since increasing the fly ash content leads to declined interfacial frictional bond and lowering the matrix toughness. Strong tensile strain capacity 3-4 % was demonstrated by all the mix design except ECC G1. ECC G2 and ECCG4 outperform the reference control mix ECC R0 in terms of strength, even though ECC R0 has high OPC content. It is also found that first cracking strength of all the mix design has higher value than that of reference ECC R0.

Compressive strength of ECC mixtures up to 8 months are summarized in Figure 2.2. G1 to G4 has same amount of cement content, hence its exhibits similar strength gain rate , 3 days strength was observed 12 MPa, at 28 days G2 and G3 crosses 35 MPa. Mixture ECC G4 gained slow strength than G2 with fly ash, and ECC G1 defeat similar mixture with advantage of reactive ash. These ions forming strong interphase thin layer between PVA and cement grain, Al^3 exists in form of C_3A and C_4AF and reacts with gypsum and form sulfo-aluminate hydrates. Specially buildup $Ca(OH)_2$ in surface of PVA. But in Fly ash $Al^{3+}$and Ca^{2+} are not free and dilute the concentration of these cations in matrix which reduce the possibility of forming strong chemical bond between PVA and cementitious matrix because of the sulfo-aluminate, in fact Ca(OH)2 is responsible chemical bond. The second mechanism contributing to interface property changes which is aggregation of inert particle on PVA fiber surface, amorphous carbon. Class F has high carbon content than of class c due to residual LOI. It is noticed fiber have been washed out from from fresh ECC mixes having high volume fly ash (Class-F). XEDS analysis proof that carbon content concentration is noticeably higher than virgin fibers. A fiber has been pull out from matrix even though no coating is there. It is evident that carbon tends to accumulate on the PVA during mixing give lubrication for Pullout. Mechanically, carbon coating helps to reduces frictional stress, and shall weaken chemical bond.

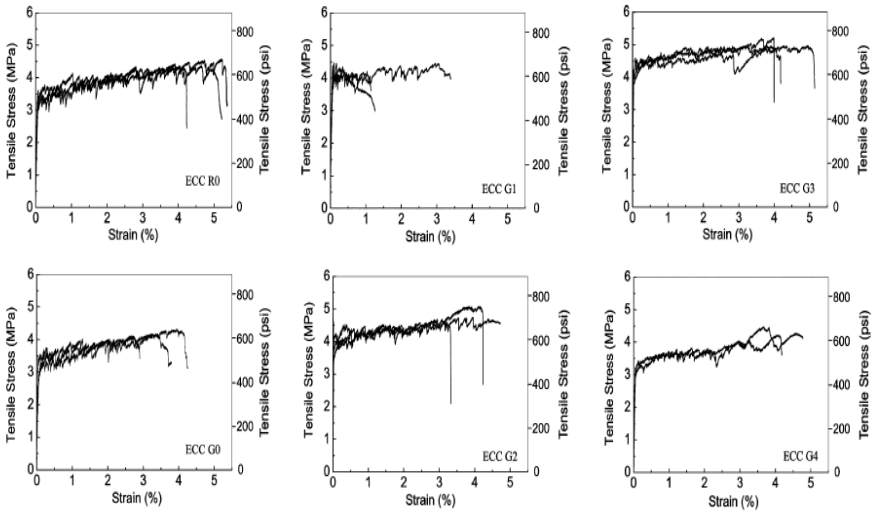

Figure 2.1 Tensile Behavior of ECC Mixture Containing Ample Ash Content (Wang and Li, 2007)

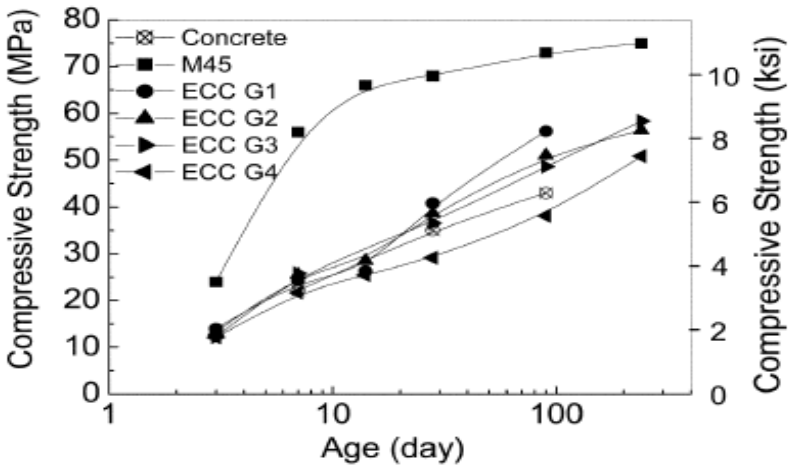

Figure 2.2 Comparison of 8- Month Compressive Strength Developed of Green ECC Mixture With Normal Concrete (Wang and Li, 2007)

Mixture ID	First cracking strength(MPa)	Ultimate Tensile Strength, MPa	Tensile Strain capacity, %
ECCR0	2.92	4.41	4.88
ECCG0	3.3	4.14	3.41
ECCG1	3.8	4.23	1.54
ECCG2	3.69	4.8	3.9
ECCG3	3.92	4.77	4.29
ECCG4	3.08	4.35	3.95

Table 2.2 Tensile Properties of ECC Mixture (Wang and Li, 2007)

Zhou et al. (2010) investigate the study of ECC with lime stone powder and BFS. Silica sand and fly ash been totally replaced by this industrial byproducts. Different mix proportions of constituent were used to form designed and experimentally analyzed by changing the limestone powder content and BFS. Table 2.3 illustrates the designed combination of ECC mixture with different proportion of constituents. Four point bending test, uniaxial tensile test and compressive strength has investigated. The aim of this study is to make wide use of ECC made up of only two indigenous materials based matrix. Six coupon samples of 240 mm x 60 mm x 10 mm were to be cast, further sliced into four parts of 120 mm x 30 mm x 10 mm dimensions and tested for bending.

Table 2.3 Material Proportions For The Mix of ECC With Portland Cement, Limestone Powder and BFS (Zhou et al. 2010)

Mix ID	CEM I 42.5 N	Limestone Powder	BFS	W/P	Super-Plasticizers	PVA fibers (by Volume, %)
M1	1	0.8	1.2	0.27	0.025	2
M2	1	1.5	1.2	0.27	0.023	2
M3	1	2	1.2	0.26	0.018	2
M4	1	3	1.2	0.26	0.018	2
M5	1	2	1	0.26	0.018	2
M6	0.6	2	1.4	0.26	0.020	2

The compressive strength of ECC was evaluated after 28 days summarized in Figure 2.3. As we seen result of M1 compressive strength is in decreasing trend with increasing limestone ratio. Mix M5 and M6, the elevated substitution of cement with BFS, creates a reduction in strength compared to M3 and M4. All mixes have a higher compressive force of 38 MPa, which falls within the necessary ECC parameter..

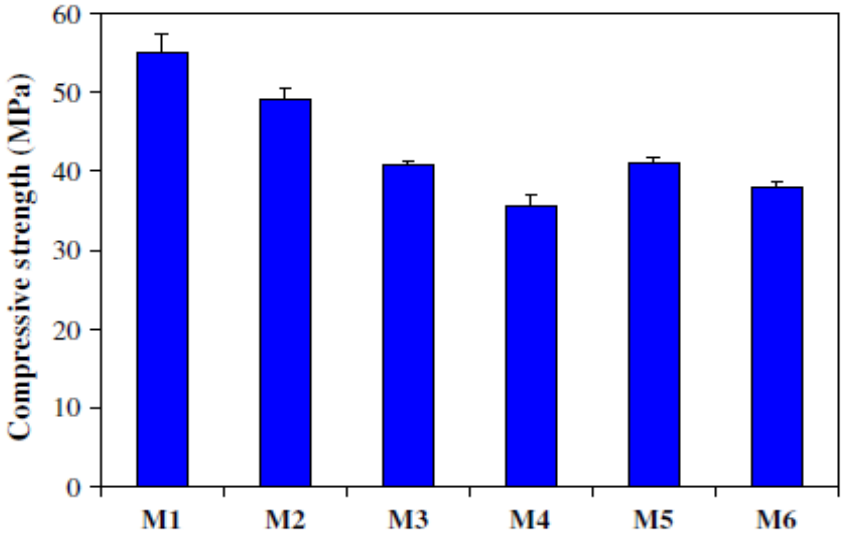

Figure 2.3 Characteristic Compressive Strength of ECC at 28 Days (Zhou et al., 2010)

Under uniaxial tensile load, M6 outperforms tensile properties; however totals powder weights in M6 it is least among rest mix, which is equal to the cement content in the normal concrete. Figure 2.4 clearly tells the tensile stress vs strain curve of M6. Tensile test has been calculated by mean result of four specimens which is 3.3% respectively. Figure 2.5 summarizes ECC's tensile strain ability with BFS content and calcareous powder content. From M1, as the calcareous material first increased the ability of the tensile strain and then decreased. From Large to small M3, M4, M2 and M1. M1 shows small strain capacity of 1.7% only, but it is much higher then normal concrete. Lower tensile strength of matrix resulted from increasing limestone which is inert filler material. Besides, limestone powder exhibit low hardness, large limestone powder are cracked easily hence crack crosses large limestone powder. Therefore adding limestone powder decreased matrix toughness, aided to decrease first cracking strength. It is suggested that descending toughness of composite matrix is favorable for increasing ductile property of ECC composite. On the other hand excessive addition of limestone has negative effect in strain-hardening property. M3 contained optimum amount of limestone.

Figure 2.5 shows M5 and M6 show higher strain capacity in tension is 3%. The decreased PE/BFS ratio result improved tensile strain capacity. This featured to low matrix toughness and good fiber matrix interface since BFS inclusion.

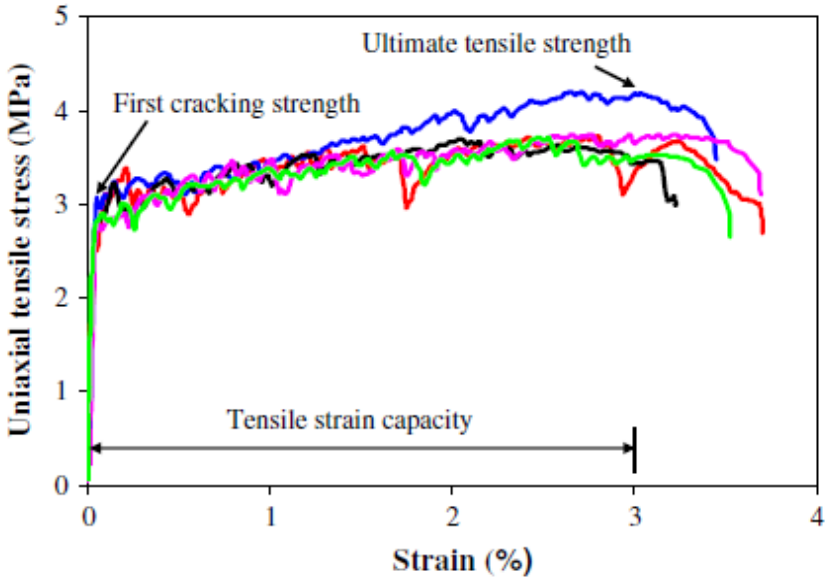

Figure 2.4 Tensile Stress Vs Tension Strain (Zhou et al., 2010)

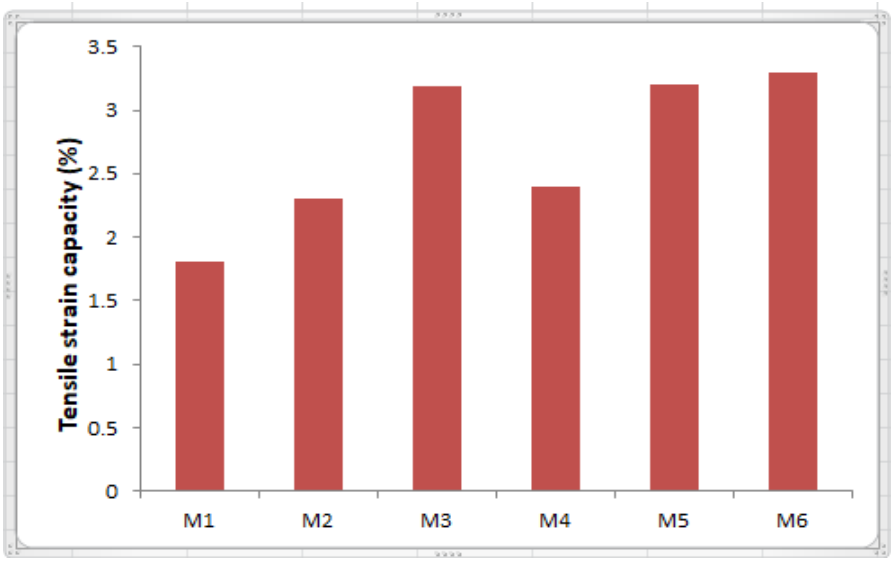

Figure 2.5 Tensile Strain Capacity of Various ECC After 28 Days Curing (Zhou et al., 2010)

Kim et al. (2007) studied the effect of ground granulated blast slag (GGBS) on ECC composite. To study strain-hardening behavior of the composite, direct tensile tests were conducted. An optimized Slag-ECC mixture proportions was found shown in Table 2.4. This was using micromechanical principle. The proportioning of matrix range was determined through bridging analysis of fiber results and workability. Ductility and tensile strength 3.6% and 5.2 MPa respectively of the Slag-ECC were observed which is higher in values than the ECC without slag. The mixing layout of ECC with slag particles outcomes in a tiny Jtip value of the same proportion of W / B relative to the blend without slag. Accordingly, ECC prepared with slag performs a higher toughness ratio than ECC without slag at the same W / B ratio. When fly ash was substituted by slag particles, considerable strain-hardening conduct of ECC is observed, as the toughness ratio has direct relationship with multiple cracking in the composite which is conducive for steady crack prorogation and conducive in behaving strain hardening. It was observed the toughness ratio (J_b/J_{tip}) decreased as slag particles added at a W/C (60%) and helped to increase tensile Strain capacity of ECC by 50%. This was mainly because of fiber dispersion behavior due to involvement of slag. Better fiber dispersion evolves from enhanced workability of fresh composite.

Table 2.4 Selected Mix of Compositions (Kim et al., 2007)

Cement	Water	Fine aggregate	Slag	HRW	HPMC
1.0	0.6	0.8	0.25	0	0.001
1.0	0.48	0.8	0.25	0.02	0
1.0	0.35	0.8	0.25	0.03	0
1.0	0.60	0.8	0	0	0.001
1.0	0.48	0.8	0	0.02	0
1.0	0.35	0.8	0	0.03	0

Faiz and Hirozo (2006) investigated the durability properties of ECC composites. The tested result shows that SHFRCC exhibits very good durability properties. The SHFRCC specimens closely spaced multiple micro cracks occurred with crack widths of approximately 0.060 mm, Under hydraulic head test permeability is checked. The result shows a noticeable increasing trend of permeability proportion to increasing crack width and steel bars resists toward corrosion. The small width of cracking, narrow the path of water movement and chloride permeability which decreased down the rate of corrosion of steel.

Mechtcherine et al. (2009) investigated strain hardening property of cement composites when subjected to cyclic tensile loading. Uniaxial tensile tests performed on unnotched, dog- bone shaped prisms total fibers contains 2.25% by volume of polymeric fiber were experimented with both a deformation and load control testing system. Table 2.5 shows the materials mix proportion for SHCC.

Table 2.5 Mix Design of SHCC (Mechtcherine et al., 2009)

Cement Kg/m3	Flyash Kg/m3	Silia sand Kg/m3	Water Kg/m3	SP Kg/m3	VA Kg/m3	PVA Fibers Kg/m3
321.0	749.1	535.0	334.5	16.6	3.2	29.3

In the deformation controlled regime, the repeated loading caused a decrease in the tensile the monotonic tests. However, no considerable effect on the strain capacity of the material was noticed for the relatively small number of loading cycles applied. There was no impact observed on the strain capacity from repeated loading cycles operated load control. The number of cracks, as well as the crack widths, as found on the specimen's surfaces did not vary much with applied different loading conditions. The cracked specimens tested under the load control regime were more prone to failure at small strain levels. The tensile strength results of the specimen are shown in Table 2.6 below.

Table 2.6 Compressive Strength of SHCC (Mechtcherine et al., 2009**)**

Type of loading	Tensile strength f_t (MPa)	Strain capacity y εtu (%)
Monotonic, deformation Controlled	3.6	2.5
Cyclic, deformation Controlled	3.9	2.4
Cyclic, load controlled	3.4	2.4

2.2.2 Literature review on retrofitting of beam column joint

Fischer et al. (2002) A research study focusing on the effect of replacing weak conventional concrete column members with engineered cement composite (ECC) was conducted. They researched the efficiency of enhanced composite ECC members under inverted cyclic loading circumstances under displacement regulated patterns. Lateral displacement rose up to 6% drift. And to maintain balance in the column 15 % of total compressive capacity of section is applied in column capacity of the T-beam. Total 4 different -beams were tested namely S1, S2, S3 and S4. First two S1 was steel reinforced column, S2 represents FRC reinforced concrete column, S3 for steel reinforce ECC column and S4 represented FRC reinforced ECC columns last two types of columns did not contained transverse reinforcement. The flexural behavior of steel reinforced ECC was stable in post yield region and deformation behavior and greater deflection capacity. The flexural stiffness of S3 is quite lower than S1, because more flexural cracking formation and lower modulus of ECC in S3, which make S3 more complaint column member. In post yielding region, S1 exhibits composite damage because of bond splitting and immediate cover spalling leaded to reduced flexural resistance and composite deterioration in plastic hinge region by increasing shear cracks. In contrast, S3 maintain the overall integrity in flexural deformation mode and column base. Reason of observed integrity was compatible inelastic deformation between ECC and steel which reduces bond stress and bond splitting and cover spalling. ECC exhibits shear resistance property and aided to preserved composite action between ECC and steel which further convert inelastic compressive deformation into ductile, In compression between S1 and S3, In hinge region of S3, performs composite behavior hence structural maintain stable inelastic deformation due to composite action. The ability of structure member undergoes inelastic deformation expressed by ductility factor, which is defined as the ratio between deflection of members in load that is 85% of peak load and deflection at yielding of tensile reinforcement. S1 exhibit ductility factor 4 where as S3 shows factor 10. It is observed that S3 (Steel/ECC) contribution toward energy dissipation is almost equal to brittle concrete, even though ductile deformation behavior of ECC, S1 has slightly higher equivalent damping ratio then S3 at small drift prior to yielding.

Chidambaram et al. (2015) investigated the behavior of joints with various composite under dynamic loading. Composite materials are ECC-reinforced PPE fiber and hybrid cement composite (HCC) with three distinct kinds of hooked steel fiber, brass-coated steel fiber and PP fiber.. The load deflection curve, ductility response, crack patterns, energy dissipation, and

damage index level of six T-beams analyzed and check with the conventional specimens under same cyclic loading. Six different types of specimens all the specimens are reinforced with four numbers of 12 mm dia in column and 3 numbers of 10 mm dia at top and bottom of beam. SJ2 had small difference in transverse reinforcement detailing that of 50 mm c/c spacing of links in hinge region and 100 mm c/c in rest. All the five specimen has similar reinforcement configuration of 6mm dia of bars and 100 mm c/c spacing throughout. Joint of six specimens are cast with different composite materials. S1 and S2 are cast with conventional concrete, S3 with steel fiber reinforced composite (SFRC), S4 with Engineered cementitious composite contained polypropylene fiber of 3% of total volume, S5 has HSF reinforced engineered cementitious composite (HECC) where HSF means hooked end steel fiber. HECC composed of 1.5% of polypropylene fiber and 2% hooked end steel fiber. S6 has composite name BSE Engineered cementitious composite (BECC), where BSE stands for brass coated steel fibers. It has composition of polypropylene 1.5 % by volume and 2% of BSF in volume. The hysteresis behavior of S4, H-ECC in joint specimen was noticeable than rest of HPFRCC specimens including conventionally confined joint specimens. Hybrid Cementitious Composites maybe a good option in shear deficient member to enhance performance under earthquake load. The load vs deformation performance of HPFRCC joint specimens shows major impact elastic and inelastic performance. The post yield and ductility capacity of S5 (H-ECC) joint specimens are almost 2 folds more than that of S2 confined joint specimens. It is noticed that different types of HPFRCC joint specimens can helps post-yield capacity of the joint.

The strength loss and stiffness decreasing of S2 and SFRC S3 specimens exhibits that the peak load is increased about twice than yielding load of other T-beams in after yield region drift ratio. Only 40% of load carrying capacity is viewed after drift increases 150%. in conventional specimens, after attaining the peak load. After peak load over post-elastic drift expands by 300%, a considerable decrease in stiffness is noted around 60% of the load ability. However, reduced pattern is seen gradual in case of S3 specimen as compare to S2. Horizontal wide spread cracks and diagonal shear cracks cracks in joint region attributes uniform dissipation of energy mechanism of HPFRCC joint specimens dissipated energy uniformly. It can be clearly stated that the specimens containing HPFRCC is three times more ductile than controlled confined specimens. Hybrid composite exhibited higher damage tolerance capacity as compare to distinct fiber composite.

Sharma and Bansal (2018) Investigate the efficiency performance of retrofitted ultra-high-performance hybrid composite fiber strengthened (UHP-HFRC) in the outer beam column joint. Four control beam column joints were evaluated in different damage index levels under quasi-static cyclic loading- slightly damaged; mildly damaged; severely damaged; and completely damage and theirs cross ponding damage index value are damaged 0.3, 0.45, 0.75 and 1 respectively. All the damaged T-beams retrofitted by UHP-HFRC. Various parameters were studied and compared the performance in between specimens in the experiment. Highlighted parameters were observed thoroughly. Characteristics of controlled and retrofitted joints are compared, strength, stiffness degradation and energy dissipation. It was observed that UHP-HFRC has better performance in the joint zone distorted initially in lower damage index; slightly damage and moderately damaged. Therefore, gradual drop of peak load took place in the specimen. Improved ductility behavior of R-CD, R-SED, R-MD and R-SD by 20%, 21.17%, 40.29%, 45.29% respectively compared to controlled C-CD samples. It found that peak to peak stiffness is almost three times higher in retrofitted UHPHFRC specimens than controlled. Hence peak to peak stiffness is the line joining peak point reached negative and positive direction in cycle of load. Furthermore, stiffness was found increased for specimens previously damaged in moderately and slightly after retrofitting. In contrast, specimens damaged in completely and severely not found improved in higher drift ratio. Performance peak to peak lateral stiffness of all measured samples in R-SD > R-MD > R-SED > R-CD. It was seen from the experimental analysis retrofitted specimens were able to retain strength in the slightly and moderately damaged specimen as compare to severely and completely damaged retrofitted specimens. Energy dissipation capacity was found more suitable for moderately and slightly damaged structural element in higher drift ratio. R-SD and R-MD dissipated 8894KN-mm and7452 KN-mm, but found lower dissipated energy in R-SED and R-CD 5665 KN-mm and 3588 KN-mm respectively. In nutshell, Retrofitting strategy of using UHP-HFRC found most efficient and suitable for slightly and moderately damaged structural element after evaluating different parameters.

Yuan et al. (2011) perform the experimental study on total of six specimens, four RC/ECC joints specimens and two normal reinforced joints. All joint specimens are all ‘T’ types. All specimens are designed under the principal of “weak joint and strong component” to study the behavior of joint S1, S2, S3 total four specimens designed for test the study. Specimen S1and S2 are controlled normal specimens no stirrup contained, but two links in joint zone, S3 and S4 are

stirrup-free ECC / RC specimens, but two stirrups in the joint area. S5 has comparable details of reinforcement as S4 samples, S6 specimens containing ECC with reinforced concrete T samples with three shear reinforcement in the joint field.

Concrete and longitudinal steel reinforcement takes shear force in specimen S1, shear force and compressive stress leads toward premature cracking of concrete for specimen S1. The pinching function of the hysteresis curve showed that the specimen had a fragile failure behavior in S1. In comparison of S2 with S1 it is stable, and no pinching effect noticed in subsequent cycle. Stability was achieved because of detailing joint zone. It further improves shear strength and compressive confinement strength of concrete. S4 has 16.7 % higher than S2 as ECC and stirrups present in joint region. Flexure moved from shear and plastic hinge growth column base for specimen S2 and S4 failure mode, investigated from the experiment. S-5 and S-6 load vs displacement curves are comparable to S3 and S4 specimens.

Said et al. (2016) investigated the study in lab, cyclic hysteresis testing conducted for two exterior beam column joint specimens. Normal concrete (NC) is used to cast the first specimen and other specimen casted by (ECC) reinforced by PVA fibers 2% by total volume in the joint zone. Figure 2.6 from load vs displacement curve pinching effect has shown in normal concrete specimen, loops are getting small due to brittle nature of concrete shows in Figure 2.6 b. In contrast, ECC specimen Figure 2.6 b loop area of curve is big and more regulated in ECC specimens than the loops of NC specimen having small pinching effect.

In addition, the ECC's envelope curve has a wider area than the normal concrete. Consequently, Replacing the NC with the ECC in the joint zone could be a better option for enhanced parameters such as load capacity, shear capacity, damage tolerance, ductility and energy absorption capacity by replacing normal concrete with ECC. It is reproached at the early charging point that the NC joint's energy absorption capability is greater than the ECC Figure 2.6. In higher drift ratio the polymeric fibers play bridging action across cracks and start to catch them. Because of this fiber bridging action, this ECC property helps to improve the capacity of tensile strength, shear strength, ductility and energy absorption achieved in ECC samples. It also enables to reduce the pinching impact in beam–column joints hysteretic loops. Figure 2.6 shows that accumulated energy more than the NC joint is absorbed by the ECC joint specimens.

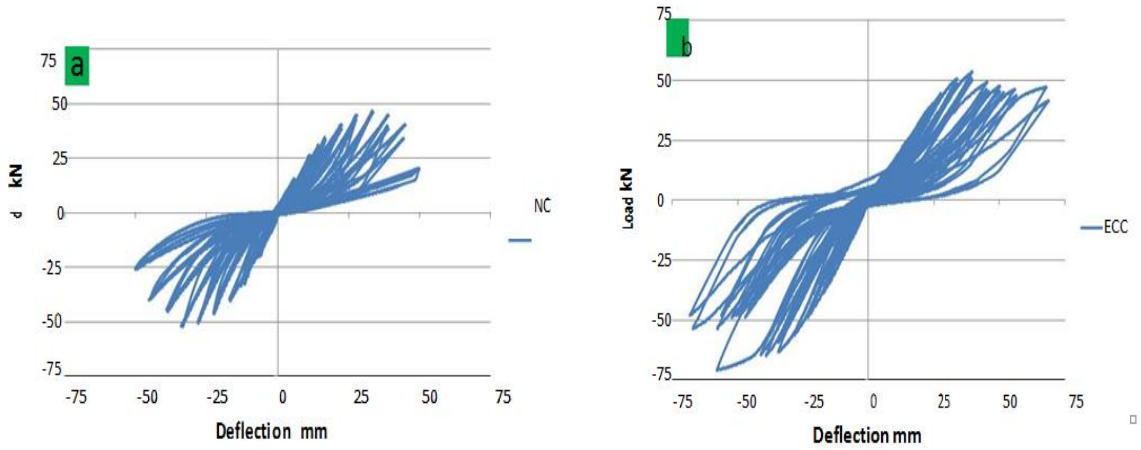

Fig. 2.6. Load Vs deflection of joints (a) NC, (b) ECC–PVA. (Said et. al., 2016)

Zhang et al. (2015) reported, load carrying capacity of specimens TJ1 was dropped, it was observed when specimens reached its peak load and further subjected to cyclic load about 4.5% due to spalling of beam and yielding of reinforcement. Although load carrying ability is reduced by some degree after peak load, successive cycles produced plateau in load-displacement envelope curve of TJ-2 and started to decrease from 2.5 percent to 4.5 percent but increased from 4.5 percent to -6.0 percent beginning to make flat load displacement curve for TJ-3 owing to enhanced inelastic conduct in plastic hinge area adjacent to the column face.

Rui Zhang et. al. (2015) It was revealed that the use of ECC composite strengthened with PE fibers improved the shear strength of the joint and helped to create plastic beam characteristics without special detailing.This was the reason behind not providing transverse reinforcement in joint for all specimens. In TJ1 first experiment performed. In TJ2 and TJ3, no transverse reinforcements in provided in beam and column thus shear capacity are almost similar. After performing the study it can imply less transverse reinforcement results better workability. Hence, Shear capacity of specimens with no transverse reinforcement but ECC is almost five times higher than the specimens with transverse reinforcement. It can be said that ECC would be better option for replacing shear reinforcement. The energy dissipation properties on the three specimens, TJ1 dissipated higher energy than TJ3 by 15%, where TJ1 has no shear detailed. TJ1 could not dissipated more energy in increased drift ration because rupture of top beam reinforcement, while In TJ2 and TJ3 smaller rupture has took place in equal drift. TJ2 and TJ3 succeed to dissipate higher energy than TJ1. TJ2 and TJ3 proofs, PP-ECC is capable of improving shear strength in joint zone. Although load carrying capacity is reduced by some

degree after achieving Stiffness degradation of all samples under dynamic loading cycle, calculated by line slope linking peak load and zero loads at half cycle at each drift, TJ2 and TJ3 perform similarly as TJ1. Although both has no shear reinforcement in beam and column. Furthermore, small stiffness degradation in TJ2 and TJ3 due to the effect of PP-ECC. Crushed PP-ECC was observed in loading test in TJ3. Equal energy dissipation and stiffness degradation is observed even after crushing of PP-ECC, it implies no effect of crushed PP-ECC.

Deng et al. (2018) experiment on the seven specimens namely S1, S2, S3, S4, S5, S6 and S7. These specimens are controlled, partially transverse reinforcement with ECC, and fully ECC composite for joint. After deep down to the experiment they found that, specimens had no or less confinement in specimens casted with ECC exhibits structural integrity. They show no wide cracks and spalling of cover found during experiment. Specimens with ECC have higher energy dissipation capacity than normal concrete that 11 to 20 %. Specimens S7 and Specimens made of ECC but no confinement exhibits higher energy dissipation than detailed and confined specimens. This was accomplished because joint integrity is preserved in the inelastic area of the beam column joint owing to elevated strength, toughness and improved energy dissipation ability of the ECC. It is also observed that ECC provides considerable factor of safety against shear stress when joint is subjected under cyclic load. ECC specimens had equal shear strength to specimens designed with transverse reinforcement, this result indicates that ECC has caliber to replace the transverse reinforcement, no shear failure in the joint area and other members attached with joints.

CHAPTER 3

DEVELOPMENT OF ENGINEERED CEMENTITIOUS COMPOSITE (ECC)

3.1 GENERAL

The aim of this work is to optimize the mixture proportions of ECC using various industrial by-products and cementitious materials. In this study attempts are taken to design ECC by replacing cement with industrial by-products. The objective is to obtain an ECC that satisfies the desired compressive strength, tensile strength and strain property.

The objective is to develop a mix with sufficient compressive and tensile strength which would meet the requirements of a strain hardening property one of the ECC's important parameter.

3.2 MATERIALS

The basic ingredients for a ECC mix are cement, fine aggregate, fly ash, fibers, superplastsizer and water. The coarse aggregates are not used in ECC mixes due to the requirement of followability. In this study GGBS and silica fume were used as partial substitute of Fly Ash (FA). The basic properties of all the materials are discussed here under.

3.2.1 Cement

IS8112: 2013 provides the specifications of OPC 43 grade. The physical properties are

Figure 3.1 OPC 43 Grade Cement Used in The Study

In accordance with the Indian standard IS: 8112: 2013, Table 3.1.

Table3.1 Engineering Properties of OPC

Characteristics	Experimental values Obtained	IS 8112: 2013 Specified Values	Test Method Referred to
Specific Gravity	3.04	-	IS 4031 part 11
Standard Consistency (%)	28	-	IS 4031 part 4
Initial Setting Time	40 minutes	30 (Minimum)	IS 4031 Part 5
Final Setting Time	320	600(Maximum)	
Compressive Strength (MPa)			
7 days	33.5	33	
28 days	44.5	44	

3.2.2 Fly Ash

Fly ash is a waste product of pulverized coal-based thermal power plants. Before discharging into the atmosphere, small particles of ash are gathered in the collection scheme as a fine powder. Particles of fly ash are spherical in form, varying from 1μm to 150μm in diameter. The fly ash used in this research was obtained from Patiala, Punjab, Rajpua energy plant. Energy Dispersive X-Ray Spectroscopy (EDS) experiment was performed to determine the fly ash's elemental structure (see Figure 3.2). Table 3.2 discusses the physical characteristics of fly ash supplied by the manufacturer itself and the chemical composition acquired from the EDS test is shown in Table 3.3. After viewing the chemical component proportions, fly ash tested can be positioned as Class F fly ash according to the ASTM C 618 standard.

Table 3.2 Physical Properties of Fly Ash (Provided by Manufacturer)

Physical properties	Value
Color	Whitish grey to grey with slight black
Bulk density	1120 kg / m^3
Specific gravity	2.36

Fineness	3527 cm^2/gm

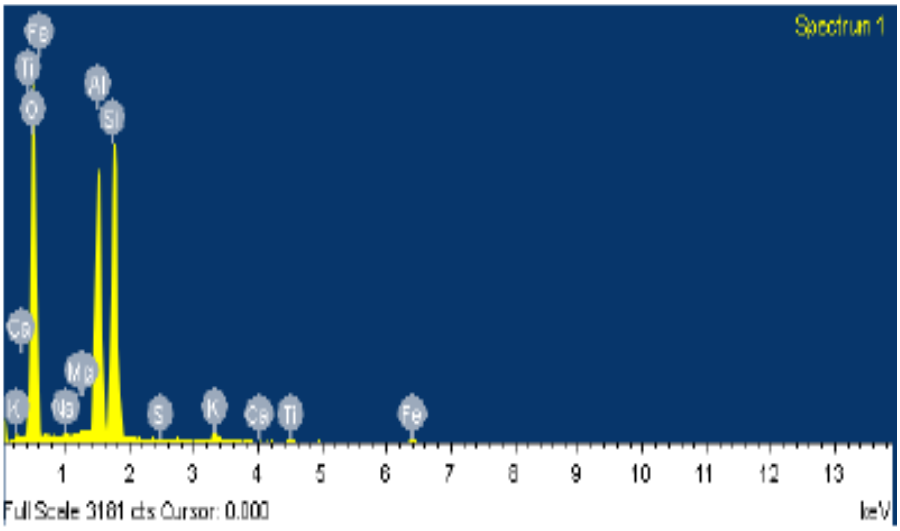

Figure 3.2 Elemental Composition of Fly Ash

Table 3.3 Chemical Constituents of Fly Ash

Constituent	Class F Fly ash (%)	ASTM C 618 (2003):Requirements
SiO_2	57.40	-
Al_2O_3	39.95	-
Fe_2O_3	0.3	-
SiO_2+Al_2O_3+Fe_2O_3	96.7	70 minimum
CaO	0.32	-
MgO	0.33	5 maximum
Na_2O	0.10	1.5 maximum

3.2.3 Ground granulated blast furnace slag (GGBS)

GGBS is the last blast furnace product in iron, copper and steel manufacturing. The GGBS used in this study is shown in Figure 3.3. The chemical components in the GGBS are presented in Table 3.4. GGBS has the particle size less then 45μm to replace cement. GGBS is generally used as pozolanic material and can be used to enhance workability and durability as a 10% to 30%

Portland cement substitute (Buokini et al., 2009).

Table 3.4 Chemical Constituents Present in GGBS.

Constituent	Composition (%)
CaO	12.40
SiO_2	73.47
Al_2O_3	4.35
SiO_2	5.48
MgO	2.14

Figure 3.3 Ground Granulated Blast Furnace Slag (GGBS) Used in The Study

3.2.4 Silica fume

It is a pozzolanic admixture that is used in elevated concrete intensity. Silica fume functions as a filler in cement vacuum. The provider of this material is KGR Agro Fusions (P) Ltd., Ludhiana Punjab. The color obtained from the silica fume was bluish gray. The silica fume particle size is about 100 times lower than the cement particle size. Table 3.5 lists the main physical characteristics of silica fume. Table 3.6 lists the chemical composition of silica fume.

Table 3.5 Physical Properties (Provided by Manufacturer)

Properties	Value
Size (typical)	<1µ m

Specific surface	15000-30000 m^2/Kg
Color	grey
Density	550-700 kg/m^3
Specific gravity	2.40

Table 3.6 Chemical Composition of Silica Fume (Provided by Manufacturer)

Constituent	Composition (%)
SiO2	92.55
Mgo	1.55
SO3	1.11
H20	0.4
K2O	2.25
Na2O	1.4
CaO	0.35
S i	0.5
Cl	0.06
Fe2O3	2

3.2.5 Fine Aggregates

In this study river sand is used. Sand has been categorized as fine sand. The sand used in the research was less than 300 um in grain size, which is in accordance with ASTM C33 (2003). The sand's particular gravity is 2.56 and 2.45 FM. The characteristics of the sand used in this job are shown in Table 3.7.

Table 3.7 Grain Size Distribution of Sand

S. No.	Experiment	Properties	Value	conforming IS Codes
1.	Grain Size Analysis	Fines, < 75µ (%)	0	IS 2720 Part IV
		Sand (%)	100	IS 2720 Part IV
		Effective size (D_{10}) (mm)	0.16	IS 2720 Part IV
		D_{30} (mm)	0.17	IS 2720 Part IV
		D_{60} (mm)	0.24	IS 2720 Part IV
		Uniformity coefficient, C_u	1.9	IS 2720 Part IV
		Coefficient of curvature, C_c	0.97	IS 2720 Part IV
2.		Classification	Sand	IS 1498-2007

3.2.6 Superplasticizers

Figure 3.4 demonstrates the admixture used in this research to create the ECC mixture. It is an sophisticated high-performance high-viscosity superplasticizer based on polycarboxylic-based technology admixture engineering admixture characteristics mentioned in Table 3.8. This product is generally intended for elevated water reduction applications and lengthy retention of workability is needed. It is free of chloride and low in alkali.

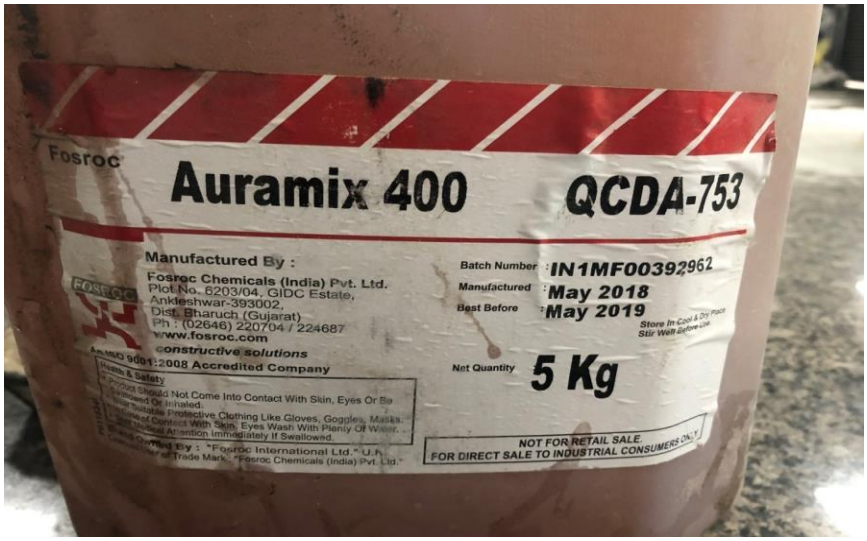

Figure 3.4 Fosroc Auramix 400 Used in This Study

Table 3.8 Properties of Superplasticizers Provided By Manufacture

Characteristic	Value
Appearances	Light yellow colored liquid
pH	Minimum 6.0
Volumetric mass @20º	1.09 kg/liter
Chloride content	Nil to IS:456
Alkali Content	Typically less than 1.5g Na2O equivalent/ liter of admixture.
Specific gravity	1.22

3.2.7 PVA Fibers

High-performance PVA (polyvinyl alcohol) fibers are used primarily in mortar and concrete. High elasticity modules, high uniaxial tensile and molecular bond strength, and resistance to alkali, UV, chemicals, high resistance to fatigue, PVA fibers are preferable to over rest fibers. PVA fibers are exceptional in their ability to create a molecular bond with mortar and concrete 300 percent greater than other fibers. Yarn Guru India, Rajasthan, purchases this fiber (see Figure 3.5). Table 3.9 demonstrates the details of the PVA fibers ' physical property.

Figure 3.5 PVA Fiber Imported From Yarn Guru India

Table 3.9 Physical Properties of Polyvinyl Alcohol Fibers (Provided by Manufacturer)

Material	Polyvinyl Alcohol
Color:	White or yellowish white
Formula	(CH2CHOH)n
Specific Gravity:	1.3
Lengths	12mm
Density	1.29
Diameter	39μm
Tensile Strengths	1100 MPa – 1400 MPa
Young modulus	25.8GPa
Hot water resistance	2.0% <
Hot water resistance	0.2%<
Absorption:	Minimal

3.2.8 Steel Fibers

The main role of steel fiber is to bridge the cracks and delay the propagation of cracks across the matrix. This capacity to stop brittle fiber composites has improved tensile strength, both at first and ultimate crack, especially under flexural loading; and even after comprehensive cracking, the fibers can keep the matrix together. The transition from a brittle to a ductile material type would significantly improve the fiber composite's energy absorption features and its capacity to resist repeated application of loading. Steel fibers are of various kinds: straight steel fibres, crimped steel fibers, and hooked steel fibers. In the present study crimped steel (SHAKTIMAN ® Steel Fibers) is used as shown in Figure 3.6 Stewols India (P) Ltd., Nagpur is the manufacturer and distribution of these fibers. The steel fibers used are specified as below Table 3.10.

Figure 3.6 Steel fiber used in ECC

Table 3.10 Property of Steel Fibers

Characteristic	Value
Ultimate strength as per ASTM A820M	>1100MPa
Diameter	0.6 mm
Length	30 mm
Aspect ratio	50

3.2.9 Linear Variable Differential Transducer (LVDT)

LVDT was mainly used in this study for measuring the deflection of compression face and tensile face of the T-Beam when cyclic test is conducting Figure 3.7 shows the LVDT used in this study. Two LVDT were used to measure the quantified deflection. This LVDT transfer data through inbuilt electric signal into data locker system from where date can be access. It has deflection capacity of 50mm maximum and minimum of 0.01mm.

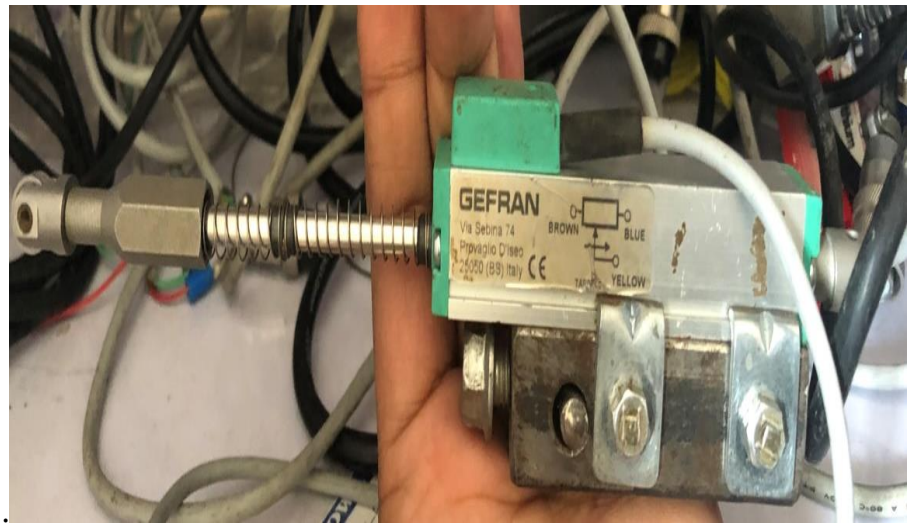

Figure 3.7 Linear Variable Differential Transducer (LVDT)

3.2 MIX PROPORTION FOR THE DEVELOPMENT OF ECC

Engineered cementitious composite was used for retrofitting of the T-Beam. (Victor Le, 2007) The initial proportions of constituents were taken from paper as shown in Table 3.11. The sand used in this research was 250 microns of medium size and was not used to exceed 300 microns. This is done by manual sieving of available local river sand. Total nine trial mixes of the design were prepared by replacing the fly ash with silica fume and GGBS in varying ratio of 10%-20% by weight is prepared as shown in Table 3.12. It is mortar based composite matrix. To make ECC more economic pozzolanic admixtures were tested in this study. Considerable cement percentage is replaced by fly ash only in the first trial. In subsequent trial Silica fume and GGBS also incorporate to improve the mechanical properties and workability. The water to binder ratio is 0.25 to 0.3 in first trials and for rest of the trial mixes W/B ratio is 0.3 remain unchanged. Three different types of fibers were used in this study; PVA 12mm, 6mm and steel crimped fibers. Steel crimped fiber was used to enhance compressive and tensile strength of the trial mixes. Main reason of incorporating silica fume and GGBS helps to achieving the tensile strain capacity attributed by improving the fiber dispersion. Silica-fume used in the mix design serves two purposes i.e. as filler which fills the gap within the cement particles and as a pozzolanic material which helps in formation of C-S-H gel by reacting CH (calcium hydroxide) which liberates in the hydration reaction of concrete. It improves the durability of the composite.

Table 3.11 Mix Proportion For The Base Mix of ECC (Mix 1)

Items	Quantity (Kg/m^3)
Cement	562
Fly ash	671
Sand (200-300 micron)	450
Silica Fume	-
GGBS	-
Superplasticizer	6.65
PVA fibers	2% by volume of concrete
Water	311.6

Table 3.12 Mix Proportions of ECC

Mix design no	Cement (kg/m^3)	PVA fiber (kg/m^3)	Steel (kg/m^3)	Sand (kg/m^3)	Superplasticizer (kg/m^3)	Water (kg/m^3)	Flyash (kg/m^3)	GGBS (kg/m^3)	Silica fume (kg/m^3)
Mix2	562	26		450	6.65	369.9	60	0	67.1
Mix 3	562	26		450	6.65	369.9	536.8	67.1	67.1
Mix 4	562	26		450	6.65	369.9	536.8	0	134.2
Mix 5	562	26		450	6.65	369.9	469	67.1	134.2
Mix 6	562	26		450	6.65	369.9	536.8	134.2	-
Mix 7	562	13	78.5	450	6.65	369.9	469.7	67.1	134.2
Mix 8	562	13	78.5	450	6.65	369.9	469.7	-	201.3
Mix 9	562	26	-	450	6.65	369.9	268.4	268.4	134.2
Mix 10	562	13	78.5	450	6.65	369.9	268.4	268.4	134.2

The sole purpose of the study is to design the ECC exhibits high compressive strength, tensile strength and more importantly achieving tensile strain hardening property.

3.3 TEST PROCEDURE

The desired properties of ECC evaluated as a part of the program- mechanical tests, tensile strain capacity and deformability. The compressive strength test was conducted to verify whether or not the blend is within the ECC strength range after 28 days. The compressive strength value must above 20Mpa. All these tests were performed for all mixes designed composite.

3.3.1 Compressive Strength

Fresh ECC mixtures were cast without compaction in 100X200 mm cylindrical moulds. After 24 hours, the hardened ECC samples were removed and placed in the healing tank for 28 days. CTM is shown in Figure 3.8. Maximum capacity of CTM machine is 5000 KN. Test of concrete has performed as per BIS 516-1959. he average compressive strengths of three identical ECC samples is reported.

Figure 3.8 Compressive Strength Testing of ECC Trial in Compression Testing Machine

3.4.2 Flow table test

Followability is the ease with which a material could be transported and placed. It can be used to evaluate the consistency of the ECC mix. If the consistence is not correct, the concrete will not have the desired qualities. Following test was performed to evaluate the deformability factor of various trials ECC mixes. The deformability of ECC can be evaluated using the slump flow test (ASTM C 230:1997). The apparatus and setup used to perform this study shown in Figure 3.9. For the test 60 mm diameter and 40 mm height cylinder was placed on a level surface. Then, the mix was poured into the cylinder the sample tamped twice in two layers. The tamping was done 20 times for each layer in a rotating motion. Then the cylinder is lifted and flow table was allowed to drop 25 times in 15 sec. The ECC subsided resulting in formation of a spread. The diameter of this spread was measured in orthogonal direction and mean of these values was considered as cylinder slump flow (see Figure 3.11).

Figure 3.9 Flow Table Apparatus Used in The Study.

Figure 3.10 Measuring Followability of Fresh ECC

3.4.3 Tensile strength

The split tensile strain equipment is used to measure both split tensile strength and tensile strain. The equipment consists of one fixed plate support in one end and movable plate unit supported spring at other end. Figure 3.11 shows the complete set up of the experiment. The dimensional detail of the setup is shown in Figure 3.12. The spring used in the setup supported a plate part to hold the LVDT for sensing the lateral deflection caused by load. The specimen along with complete setup was placed in the compression testing machine for split tensile testing. Testing is performed as prescribed as per BIS 5816-1999. The complete split tensile test is shown in Figure 3.13.

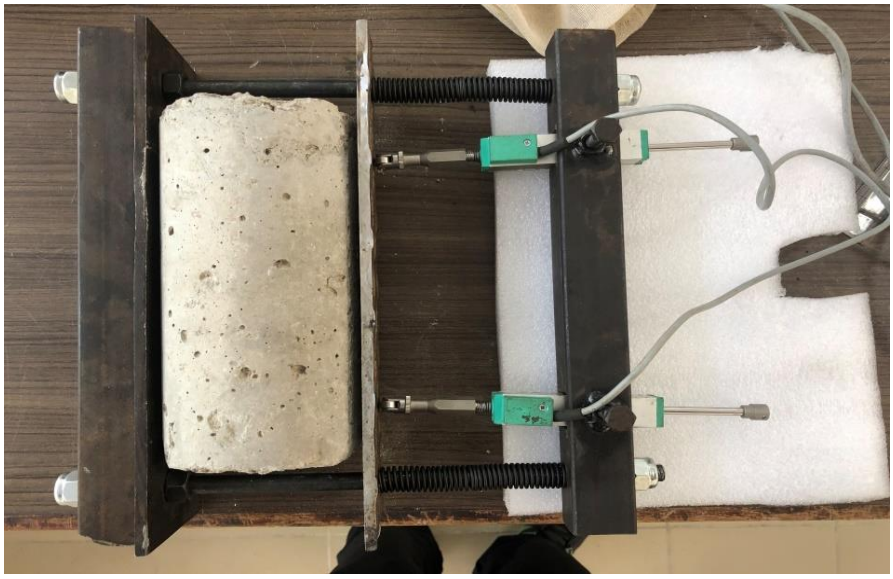

Figure 3.11 Split Tensile Strain Measuring System

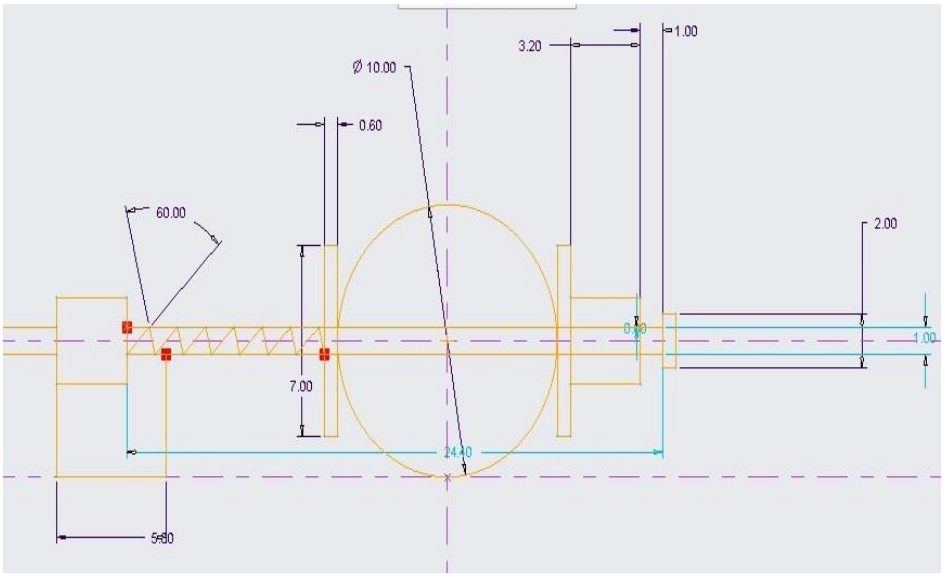

Figure 3.12 Geometric Dimension of Split Tensile Measuring Equipment

Figure 3.13 Spiting Tensile Strength and Strain Measuring in CTM

3.5 RESULT AND DISCUSSION

3.5.1 Introduction

The section deals with the results obtained for the fresh and mechanical .Three sub categories of design are formed such as control, varying industrial by product with PVA and varying industrial by product with PVA and steel fibers. The purpose was to determine the best proportion of materials that can provide the desired properties of ECC and which would further used as retrofitting material in damaged beam column joint.

3.5.2 Slump Flow

Deformability is very important parameter for self-consolidation property of ECC in fresh state. Deformability factor is denoted by (ɼ) and calculated using the following equation.

$$ɼ = (D1 - Do)/Do \quad (6)$$

D1 is average diameter of two orthogonal direction and Do is the base of slump. For good self-consolidation value of 'ɼ′ must be minimum of 2.75 (Lepech and Li, 2007). Table 3.13 listed the deformability value of all the trial mixes and the resulted value shown in bar chat in Figure 3.13.

Table 3.13 Slump Flow Test on Fresh Mixes of ECC

Trial Mix	Deformability (ɼ)
Mix1	2.7
Mix 2	2.875
Mix 3	2.7
Mix 4	2.87
Mix 5	3.125
Mix 6	3.125
Mix 7	3.125
Mix 8	3.375
Mix 9	3.5
Mix 10	3.75

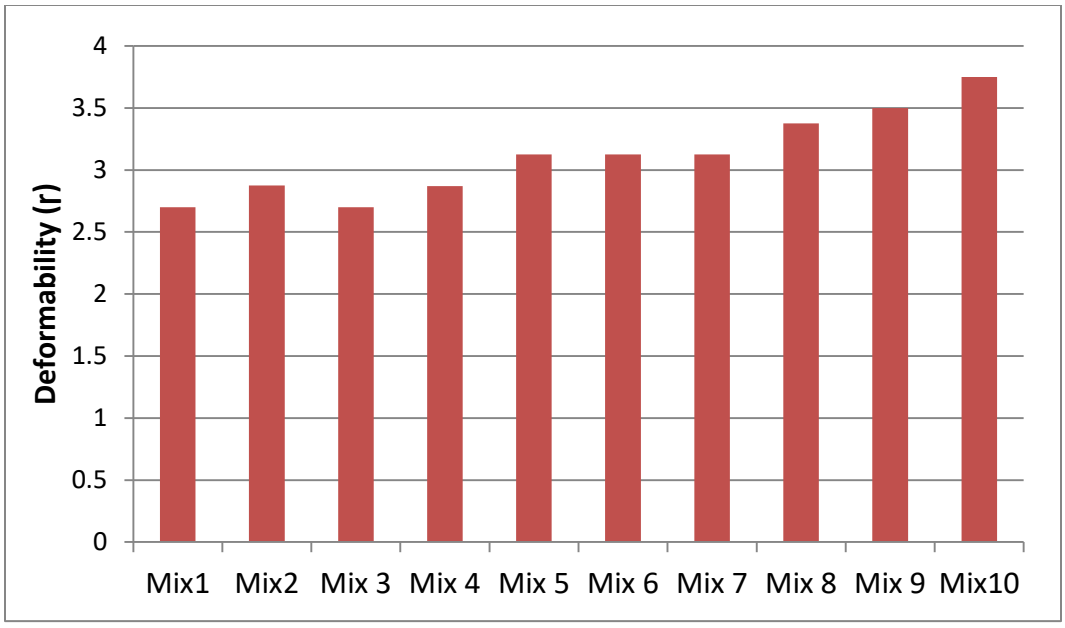

Figure 3.14 Deformability Value of All The Mix Design

It indicates that the GGBS and silica fume replacement in the ECC increase the workability. The increased workability in ECC mix is due to inclusion of GGBS and silica fume which has very fine particle size as compare to cement. The smoother texture of the surface and the glassy surface of GGBS particles also enhance the workability of the matrix. The results show that mix containing higher quantity of GGBS has shown better flow. The similar observations were made by (Soni et al. 2013).

3.5.3 Compression Test Result

The compressive strength test was carried out on the control blend Mix1 and on mixtures prepared with GBBS and silica substitutes of fly ash. The compressive strength of the different samples, measured using the compression testing machine are shown in the Table 3.14.

Table 3.14 Compressive Strength of Various ECC Mixtures in 28 Days

MIX	Compressive strength (MPa)
Mix 1	14.2
Mix 2	18
Mix 3	21
Mix 4	17
Mix 5	23

Mix 6	22
Mix 7	24
Mix 8	23
Mix 9	26
Mix 10	31.97

The compressive strength of control Mix1 has observed very less than desired. Mix 5 exhibits higher compressive strength than all of the mixtures in sub category of varying replacement of industrial by product with PVA. Total 30% fly ash been replaced by 20% of silica fume and 10% of GGBS. Compared to the blend with less proportion of GGBS substitutes, the mix comprising higher amount of GGBS has shown higher compressive strength. This rise in compressive strength owing to GGBS indicates better C-S-H gel formation relative to the fly ash mix as seen in past study results (Achtemichuk et al., 2009). This value, however, is still less in terms of ECC's desire for power.

The mix Mix 10 outperformed all the mix design since it has 1% of steel fiber and 1% of PVA fiber by volume of composite (see Figure 3.15). This improvement comes by better formation of C-S-H gel from GGBS, better fiber dispersion property of silica fume and crack bridging action help to uplift gross compressive strength of Mix 10. Furthermore, Steel fibers crack-arrest and crack-control mechanism has three main modifications in the conduct of composite-enhanced steel fibers (SFRC) (Ocean Heidelberg Cement Group, 1999); 1) Adding flexural cracking delays to SFs. The strain can be increased by 100 percent on the first crack and the ultimate strain rises by 20 to 50 times compared to normal concrete; 2) Adding steel fibers helped improving post peak behavior of concrete; 3) Crack bridging property aided to enhanced ductility gave the structure a higher ability to absorb energy (increased toughness) before failure. It is explored that Johnston (1974) and Mayfield (1971) and Dixon add up to 1.5% of SFs by volume increased the compressive strength rise by 15%.

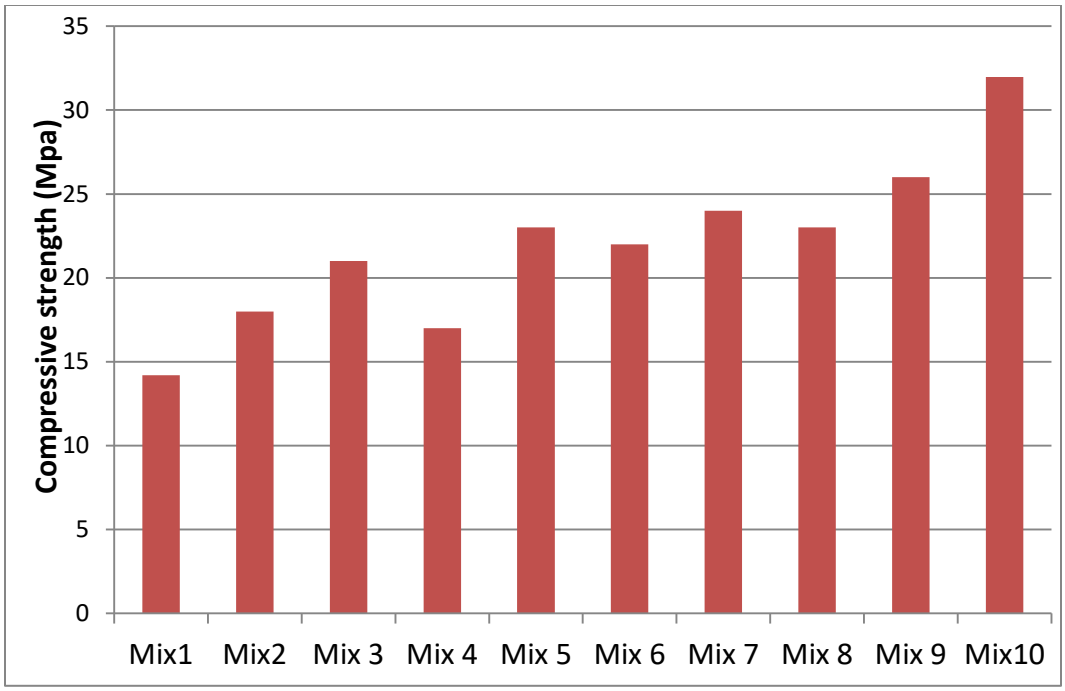

Figure 3.15 Compressive Strength of Trial ECC at 28 Days

3.5.4 Split Tensile Strain Capacity and Strength

The tensile strength of the different samples measured with split tensile strain measuring equipment and tensile strain capacity is measured with corresponding tensile strength value which is shown in Table 3.15. The Table presents the average of the values these specimens which were casted and tested, after 28 days of curing for each of the ECC mixes.

Table 3.15 Tensile Strength Variation in 28 Days of Different Mixes

MIX	Split tensile strength (MPa)	Split Tensile strain capacity (%)
M45	2.79	1.84
M 2	2.6	1.87
M 3	2.8	1.9
M 4	2.17	1.8
M 5	2.79	1.8
M 6	2.9	1.91
M 7	4.2	3
M 8	3.5	2.2
M 9	2.9	3.1
M 10	3.2	3.3

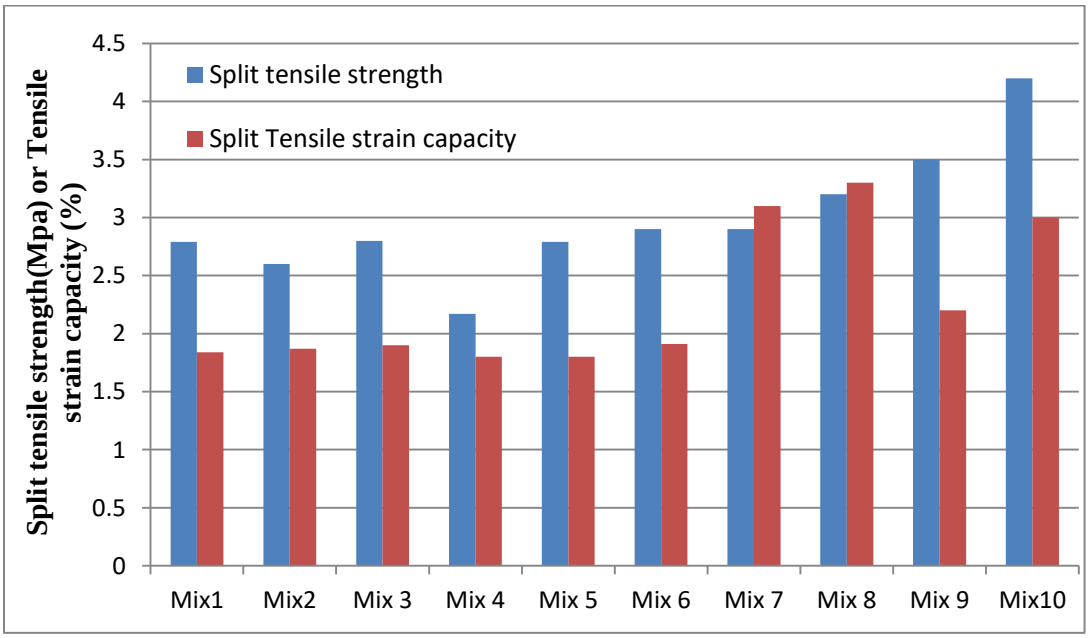

Figure 3.16 Split Tensile Strength and Tensile Strain Capacity of ECC At 28 Days

The maximum tensile strength and tensile strain capacity is achieved by Mix 10 i.e. 4.2MPa and 3 MPa respectively clearly shown in Figure 3.16. Whereas, Mix 4 has comparatively small strength and tensile strain capacity i.e. 2.17MPa and 1.8 % respectively. For the mixtures from control mix to Mix 6 no increment in strain capacity is seen even after replacing the fly ash by silica fume and GGBS. Although Mixes M7, M8, M9 and M10 exhibit increasing tensile strain capacity and split tensile capacity. After addition of silica fume and GGBS there is formation of steady state crack formation which support the ductile property of material. After adding this pozzolanic material it supposed to increase toughness of matrix which has adverse impact in strain capacity of material, but slag is expected to provide benefit from improving the fiber dispersion (Jian Zhou et al, 2009). The ratio of cement to fly ash comes down when considerable amount of fly ash is replaced by GGBS and silica fume. This replacement attributes decreasing the toughness of matrix and better fiber matrix interface; both are conducive for increasing ductility of the ECC composite. Fiber bridging strength across the cracks tends to increase the tensile load carrying capacity, which generate new cracks. If tensile loads exceed the fiber bridging strength fibers in the composite pulled out and matrix or rupture and failed ECC. Adequate fibers amount has ensured to prevent the rupture. In this study 1% PVA and 1 % steel fibers (total of 2% fibers) secures the adequate bridging strength so that composite perform well and ensures optimum strain capacity.

CHAPTER 4
EXPERIMENTAL PROGRAMME

4.1 INTRODUCTION

This experimental program concentrates on the behavior of the initially damaged beam column jointly developed cement composite. In the laboratory, the physical test of materials used to cast the beam column joint was performed. The material characteristics are described in the following parts.

4.2 MATERIALS

Cements, fine aggregates, coarse aggregates, reinforcing bars are used for casting all beam-column joints and silica sand, fly ash, PVA fibers, superplasticizers, cement, epoxy are used for retrofitting all beam-column joints. The specifications and characteristics of these materials are shown below.

4.2.1 Portland Cement

IS8112: 2013 sets out the OPC 43 grade requirements. The physical characteristics are listed in Table 3.1 in accordance with Indian standard IS: 8112: 2013.

4.2.2 Fine Aggregates

The fine aggregate used in this experimental study was locally accessible sand. The sand met the standard of Indian IS 383-1970. The water was sieved through a sieve of 4.75 mm to remove particle size higher than 4.75 mm. Table 4.1 shows the physical features of sand. Analysis of sand sieves is evaluated by IS: 383-1970 and outcomes are shown respectively in Table 4.2.

Table 4.1 Experimental Value of Fine Aggregates

Characteristic	Value
Type	Sand
Specific Gravity	2.44
Fineness modulus	2.56
Grading Zone	II
Water Absorption (%)	0.80

Table 4.2 of Fine Aggregate Sieve Analysis

S. No.	IS- Sieve	Wt. Retained (gm)	%age Retained	%age Passing	Cumulative % Retained
1	4.75 mm	7.5	0.75	99.25	0.75
2	2.26 mm	84	8.4	90.85	9.15
3	1.18 mm	167	16.7	74.15	25.85
4	600 µm	218	21.8	52.35	47.65
5	300 µm	288	28.8	23.55	46.45
6	150 µm	199.5	19.95	3.6	96.4
7	Pan µm	36	3.6	-	-
Total		1000			256.25
	Zone II				FM = 2.56

4.2.3 Coarse Aggregates

Locally collected, the coarse aggregates used in this study have a mixture of 10 mm and 20 mm in size. Different engineering properties are tested according to the guidelines for code. These 10 mm and 20 mm physical properties are illustrated in Table 4.3In Tables 4.4 and 4.5 respectively, the value obtained from the sieve analysis of coarse aggregate conducted in the laboratory for 10 mm and 20 mm.

Table 4.3 Physical Properties of Coarse Aggregates

Characteristic	Values	
Color	Grey	Grey
Shape	Angular	Angular
Maximum Size	20mm	10 mm
Specific gravity	2.61	2.68

Table 4.4 Analysis of Coarse Aggregates (10 mm)

S.No	IS Sieve	Wt.Retained (gm)	%age Retained	Cumulative% Retained	% Passing
1	80 mm	0	0	0	100
2	40mm	0	0	0	100
3	20 mm	0	0	0	100
4	10mm	1240	41.33	41.33	58.67
5	4.75mm	1640	48	89.33	10.67
6	Pan	120	4		0
Total		3000	100	134.63	FM=(134.63+500)/100 FM= 6.34

Table 4.5 Analysis of Coarse Aggregates (20 mm)

S.No	IS Sieve	Wt.Retained (gm)	%age Retained	Cumulative% Retained	% Passing (100-CR)
1	80 mm	0	0	0	100
2	40mm	0	0	0	100
3	20 mm	0	0	0	100
4	10mm	2600	86.7	86.7	13.3
5	4.75mm	385	12.8	99.5	0.5
6	Pan	15	0.5		0
Total		3000	100	186.2	FM=(186.2+500)/100 FM= 6.86

4.2.4 Water

Water is used in concrete mix design as a binding agent. Drinking water is generally appropriate for mixing and healing concrete. In this laboratory-accessible research, potable water is used to prepare concrete design.

4.2.5 Reinforcing Steel

In the beam column joint, HYSD bars of 10 mm and 8 mm diameter of Fe-500 D (Tata Tiscon) were used as reinforcement. 10 mm dia bars used for tension strengthening and 8 mm

bars are used as compressed steel. The stirrups bars of 8 mm diameter used. Table 4.6 lists the mechanical properties of steel.

Table 4.6 Tata Tiscon 500 D Mechanical Characteristics (Provided by Manufacturer)

Mechanical Properties	Unit	Conforming IS:1786 Fe 500D	Tata Tiscon Fe 500D
Yield Stress(YS)	N/mm^2	500	540
Ultimate Tensile Strength(UTS)	N/mm^2	565	600
UTS/YS	Ratio	1.10	1.12
Elongation	%	16	18

4.2.6 Nito Bond

The achievement of the reinforcement resides in the bonding strength of concrete chipped concrete layer layers and the fresh composite layer of fresh composite retrofitting. Bonding relies mainly on the epoxy resin performance used to bond ECC to concrete surface. There is a wide variety of mechanical characteristics on the market where Nito bond is used. Nito bond EP is based on pigment-free solvent-free epoxy resins and good fillers. It is supplied as a two-component material ready for on-site mixing and use in pre-weighed quantities. Binding fresh moist cemented products to existing cemented surfaces. Nito bond EP can also be used as part of a repair system requiring an obstacle to substratum/repair. Table 4.7 demonstrates the manufacturer's mechanical characteristics of the Nito bond.

Table 4.7 Mechanical Properties of Nito Bond (Provided by Manufacturer)

Mechanical Properties	Value
Compressive strength	70 N/mm^2
Tensile Strength	30 N/mm^2
Slant shear strength	36 N/mm^2
Water Absorption	0.05 N/mm^2

4.2.7 Hydraulic Actuator

Hydraulic actuator used in this study has capacity of 500KN. It was fixed in vertical plate attached with channel section. These jacks operate both in vertical and horizontally for use indifferent lifting, pushing and spreading application. In these research actuators orientation is horizontally oriented to meet the simulation of cyclic load.

4.3 DESIGN OF CONCRETE (M20)

M20 concrete mix has been intended to use cement, fine aggregate and crushed coarse stone aggregates as per IS: 10262-2009. It took as 0.50 the water / cement ratio. Table 4.8 provides the mix proportions. With this blend ratio, the cubes were prepared and tested at 7days and 28 days of age. The compressive strength of the cubes (average 3 cubes) was 18.9 MPa and 29.40 MPa at 7days and 28 days.

Table 4.8 Material Proportion For M20 Grade Concrete

Cement	Fine Aggregate/sand	Coarse Aggregates	Water
394 kg	637 kg	1142 kg	197 kg

4.4 RCC T-BEAM DESIGN

T-beam is intended using concrete grade M20 and steel grade Fe 500D in the current research. The RCC T-Beam is designed with a limit state design method and under-reinforced method (see Figure 4.1). The beam is constructed on the compression surface with 2 steel bars of 8 mm dia and 3 bars of 10 mm dia on the tension base. In column section consist of 4 steel bars of 10 mm dia bar. The beam sizes are 225 x125 mm (225 mm is depth and 125 is width) and 125 x225 mm (225 mm width and 125 mm is column depth) detailing and the real T beam joint is shown in Figures 4.2 and 4.3.

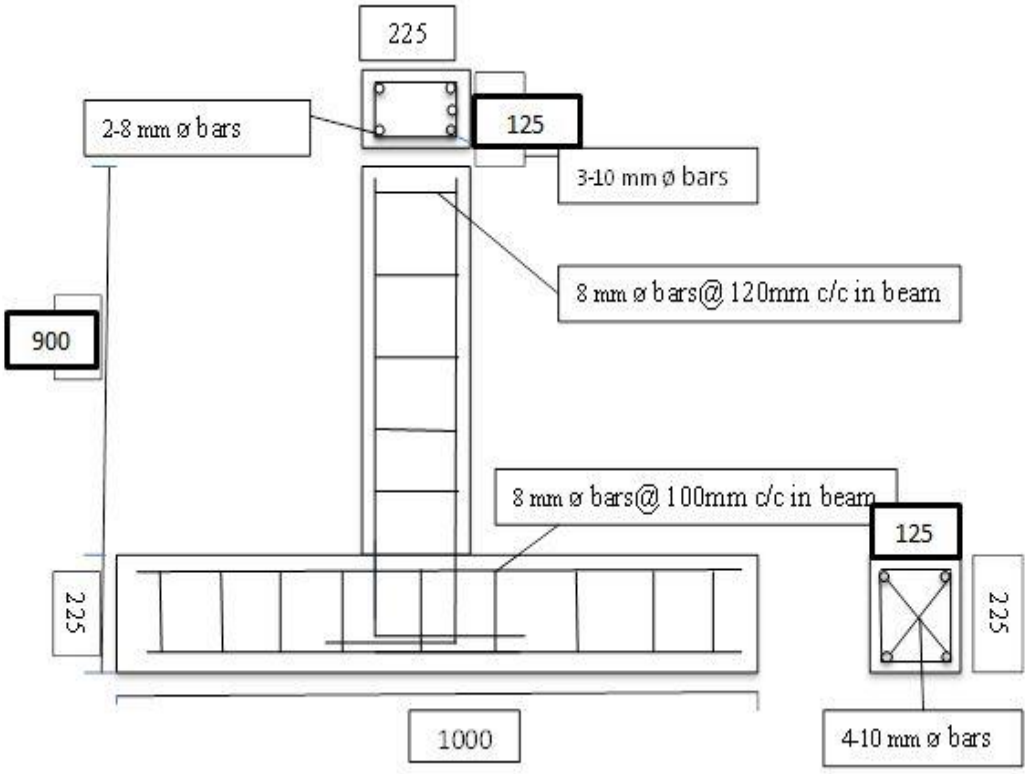

Figure 4.1 Schematic Illustration of RC Beam Column Joint

Figure 4.2 Reinforcement Detailing of Steel for T Beam

Figure 4.3 T-Beam Column Joint Specimens

4.5 CASTING OF RCC T-BEAMS

The complete T-beams mould consist of beam part and column part, where beam mould sized 225x125 mm (225mm depth and 125mm width) and column mould sized 125 x 225mm (125 mm is depth and 225 mm is width) of the mould. The 25 mm spacers are used to provide the strengthening with a standardized cover in a beam and 40 mm spacer supplied on the column cover. With the assistance of the vibrator, the bars positioned in the place according to the layout, concrete mix is poured into the mould and internal vibrations. The vibration is performed until the mould is filled and no gap remains. After 24 hours, samples are finally removed from the mold. Using jute bags, the samples are healed for 28days after demolding.

4.6 TESTING ARRANGMENT

The T-Beams were set and fixed tightly in the testing frame. Using double acting jacking, specimens are examined. It has 300KN capability Figure 4.4 displays full test setup. The technique of displacement control loading applies quasi static inverse cyclic loading. The load history is shown in Figure 4.5. In this experiment column is laydown parallel with base and column is orthogonally downed to the support. Nuts and plates are used to solve the column's two far ends 100 mm from the ends. Roller types supports are used to supports are used to support the column, placed at same0 distance where nuts and plates are tightened. The moments and deflection of columns are restricted by help of hydraulic jack and nuts and bolts in this study, since prime focus of study is only beam column joint get through rotation. The column is subjected to 10% of axial load capacity to copy gravity load of actual system. At the actuator

loading point and next to the specimen for the compression side of the beam, a linear differential transducer with a capability of 50 mm is mounted. Both the LVDT is connected to the PC based data acquisition software further computed to estimate complete strength and degradation of stiffness of the beam column joint.

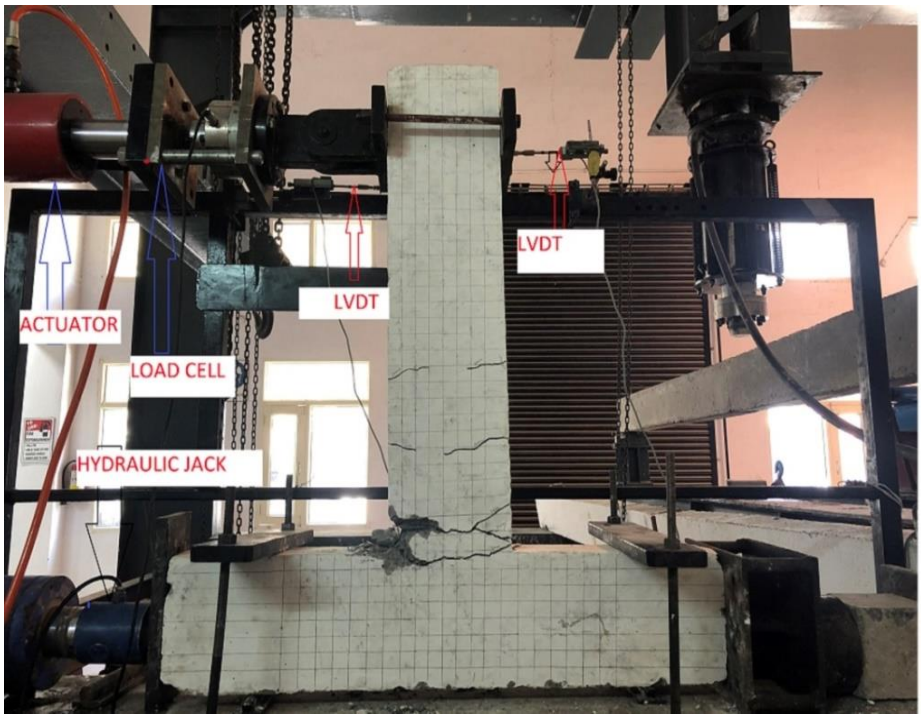

Figure 4.4 Testing Process of Beam-Column Joint

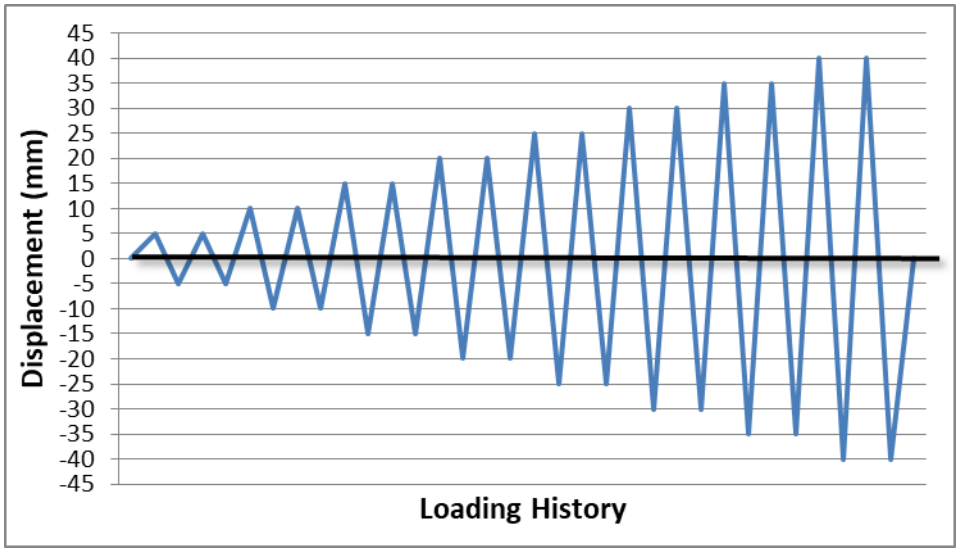

Figure 4.5 Cyclic Loading History Diagram

4.7 DAMAGE LEVEL OF BEAM COLUMN JOINT

Controlled specimens are assessed in this research under quasi-static cyclic load until the failure point. After receiving the test specimen's load displacement hysteresis curve, damaged index is calculated using the Park and index model technique (Y.Park et al., 1985).The derived equation as per this method is

$$D = \frac{\partial M}{\partial u} + \frac{\beta}{Fy\ \partial u} \int dE \qquad (7)$$

Here, the highest displacement (δu) experienced by the specimen is (Mu) and the highest displacement of the process is regarded. Integral part represents hysteresic energy dissipation of the cycle considered. Fy is the yield strength of the structures, which is again calculated from hysterisis curve of controlled specimen.β symbolize the strength degradation factor, value of β is took 0.1 in this investigation (Villemure et all. 1995). "D" is not dimensional parameter, hence its value got zero under elastic conditions. In other hand, if value of D≥1 indicates structure collapse completely. 0.1 (full damage); 0.6-0.8(significant damage); 0.4-0.6(significant damage) ; 0.4-0.2(significant damage); 0.4-0.2(significant harm). The value of calculated damage index of first control specimen is 1.13 from tested specimens. After getting the value of damage index of specimen catagorize as complete, severe, moderate, slight damage. Since first specimens D value is equall to 1.13 and it is categorize as completely damage. Table 4.9 listed the identification of the tested beam column joint. Identification are categorize as controlled and retrofitted including damage level of specimes they are subjected to cyclic load.. Controlled specimens are tested as completely damaged and moderately damaged and they are further retrofitted and applied cyclic load till reach final failure.

Table 4.9 Designation of Controlled and Retrofitted T beams

Designation	Identification of specimen
C1-CD	Controlled Specimens(Non-ductile)
C2-MD	Controlled Specimens(Non-ductile)
C3-MD	Controlled Specimens(Non-ductile)
R1-CD	Rehabilitation using ECC
R2-MD	Rehabilitation using ECC
R3-MD	Rehabilitation using ECC

4.8 RETROFITING STRATEGY

The damage concrete is chipped off from surface to depth of cover with the help of hammer and loose part swiped off by using blower. The total area concrete chipped is shown in Figure 4.6. To avoid abrupt change of plane with new ECC and old concrete, 1:8 slope is maintained at end part of chipped surface The proportion of Nito bond and hardener was on ratio of 1:0.5 mixed and applied on the chipped surface of the joint specimens (see Figure 4.7). Bonding agent prevents bonding failure between old concrete (M20) and new composite (ECC). Bonding agent ensures not occurrence of premature failure in concrete composite. After the layering of the bonding agent specimen has been completed, the ECC is squirted around the side of the beam and column on the chipped area. (see Figure 4.8). After completion of the retrofitting work with ECC it took out and demolded after 24 hours. The gunny bags are used for curing purpose after demolding. Specimens were fully covered by jute bags watering on the bag to balance hydration process till 28 days.

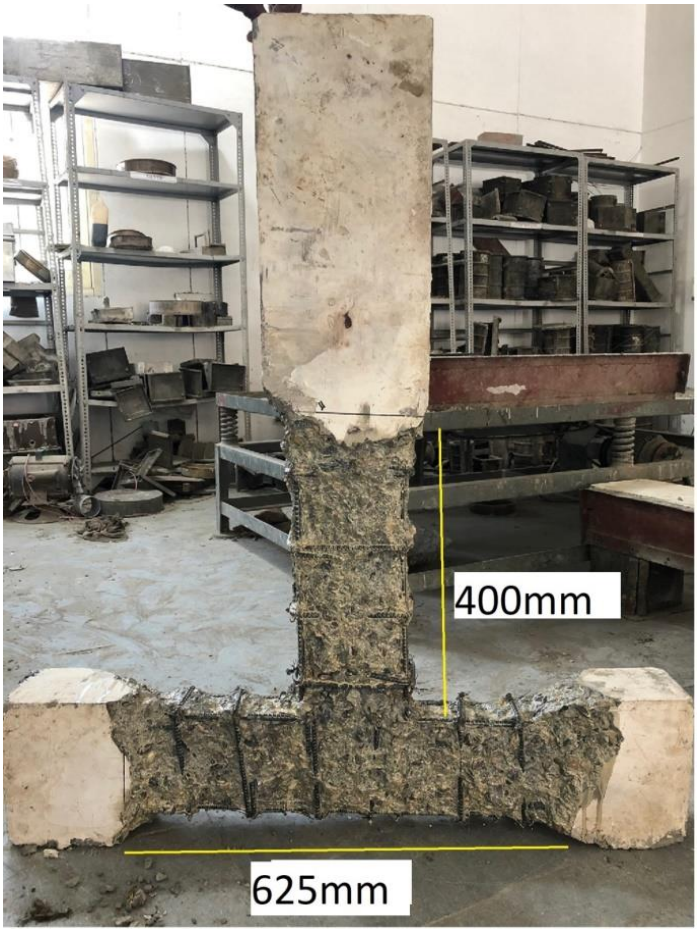

Figure 4.6 Geometric Dimension of The Chipped Area to Retrofit BJC Specimen

Figure 4.7 Nito Bond Layering on The Beam Column Chipped Surface Joint

Figure 4.8 ECC Poured in Chipped Specimen Surface Placed in Form Work

CHAPTER 5
RESULTS AND DISCUSSION

5.1 INTRODUCTION

The reaction of controlled and retrofitted specimens to evaluate the load applied versus the displacement envisages a retrofitting strategy to use ECC. This research offers insight into the strength, rigidity, dissipation of energy and joint ductility. In addition mode of failure and crack patterns are also discussed.

5.2 CYCLIC BEHAVIOR OF T BEAM

The specimens are subjected to the cyclic load as per testing protocol. It is subjected to displacement from 5mm to 35 mm, every single displacement consisting of two cycles shown in Figure 5.1 The Displacement is applied through actuator which is operated by the help of power generator (manual). Before conducted the testing, it need to ensure the first initial measure point in the scale to ensure displacement. The calculated applied load in column to simulate the gravity load is 60KN in this study. This axial load in vertical member remains equal throughout all the T-specimen study.

5.2.1 Cyclic Behavior of Controlled Specimens

The C1-CD represents the specimens first tested in QSRCL till complete damage. Behavior of specimens is presented in Figure 5.1 and 5.2 in terms of load vs displacement. From the hysteresis response curve it is noticed that after 15mm positive displacement peak load starts descends in positive displacement (push) and no peak load degrade in negative cycle of displacement (Pull). During positive displacement cycle, In 25 mm displacement load got dropped suddenly, but peak load started small rise afterward subsequent cycles and maintained load, this was due to extra two stirrups provided in the joint zone. More or less no peak load degradation has found in tension side of the beam, it is clearly visible from Figure 34 This sustained load carrying capacity increasing cycle is directly attributed due to 3-10mm dia of bars in tension phase including shear reinforcement in the joint zone. Damage index of three beam columns joint are calculated using Park and Aug method. The primary damage index is split into four levels ; full damage (CD), serious damage (SED), mild harm (MD) and slight harm (SD) is calculated using the T-beam load hysteresis curve. T-specimens are exposed to quasi-static cyclic load resulting in severe, mild and slight damage showing the damage index of that specimen. The first specimen causes severe damage at a displacement of 35 mm.

Table 5.1 Damage Index Level of Controlled Specimens

Sr. No	Specimen ID	Damage Level	Damage Index	Calculated damage Index
1	Controlled complete damage (C1-CD)	completely damage	≥1	1.13
2	Controlled Moderately damage(C2-MD)	Moderate Damage	0.2-0.4	0.47
3	Controlled Moderately damage (C3-MD)	Moderate Damage	0.2-0.4	0.47

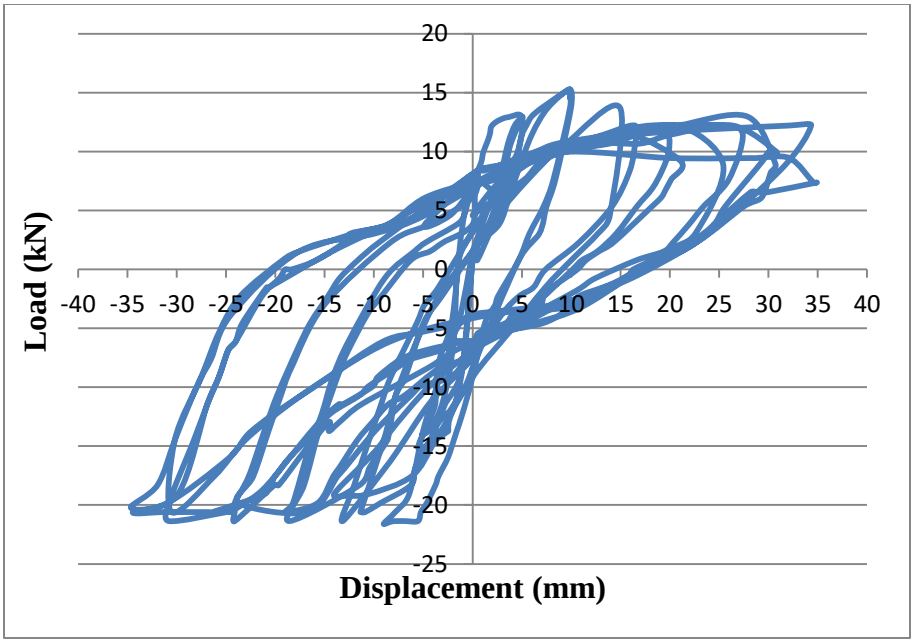

Figure 5.1 Load Vs Displacement Curve of Control Complete Damaged (C1-CD)

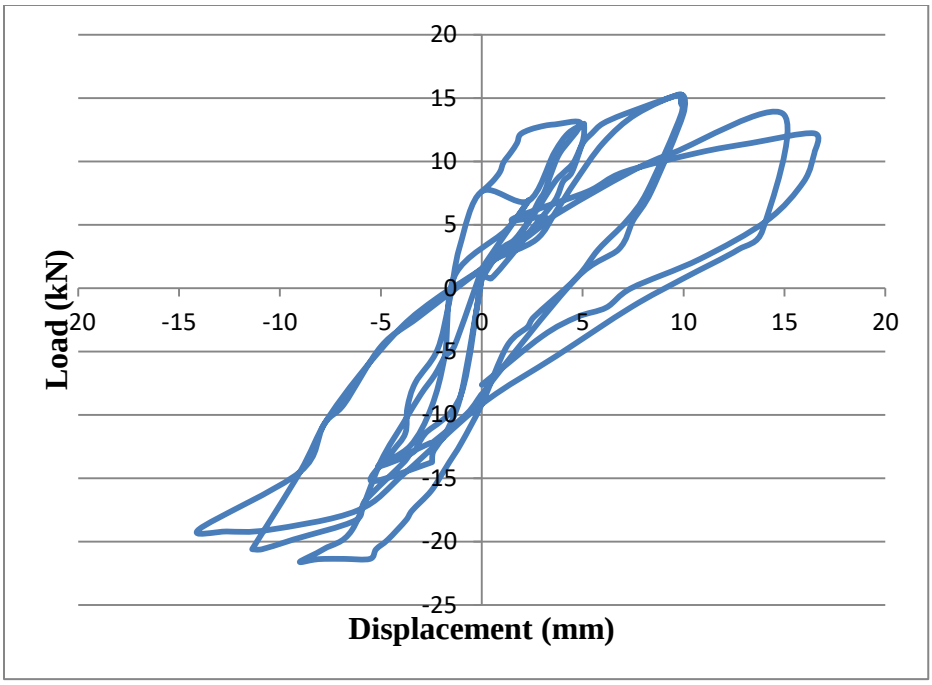

Figure 5.2 Load Vs Displacement Control Moderate Damage (C2-MD)

5.2.2 Cyclic Behavior of Retrofitted Specimens

Initially damaged, complete and moderate samples are retrofitted with ECC and 28 days of water cured. The load vs displacement of R1-CD and R2-MD are shown in Figure 5.3 and 5.4. It is observed from hysteresis curve that the ECC as retrofitting material helps to sustain the load in compression zone, even though yielding of the reinforcement already took place. The R1-CD specimens has peak load capacity of 5.94 kN in positive displacement (compression zone) where as C1-CD has 17.68 KN, which is 67 % lower at positive displacement to C1-CD, where as in tension face R1-CD goes up to 22 kN slightly higher then C1-CD. Despite of all both C1-CD and R1-CD achieved failure in compression by positive lateral displacement. After 10mm cycle peak load dropped suddenly from 5.94 kN to 1.9 kN, since reinforcement yielded initially in compression face. It leads to formation of small cracks due to inability to bridge the crack by small fibers. After this point steel fibers come to bridge the cracks but failed after 20mm displacement. After 20 mm displacement confinement provided by ECC in beam column joints no more effective and resulting in beam failure.

In R2-MD, small drop of peak cycle load is observed at 15 mm cycle it's from 15 kN to 11.5 kN as shown in Figure 5.4. It is noticed that there is considerable improvement in positive displacement and no possibility of early age failure of beam column joint. During the tests no sudden drop of peak cycle load is noticed in positive displacement cycles. Ultimate displacement

is increased; its reached up to 40 mm. Tensile ductility property of ECC helps tension load carrying capacity of specimen in both tension and compression zone, which attribute to crack control in post peak zone. Even distribution of fiber improves the ductility of material which increases overall ductility of specimen.

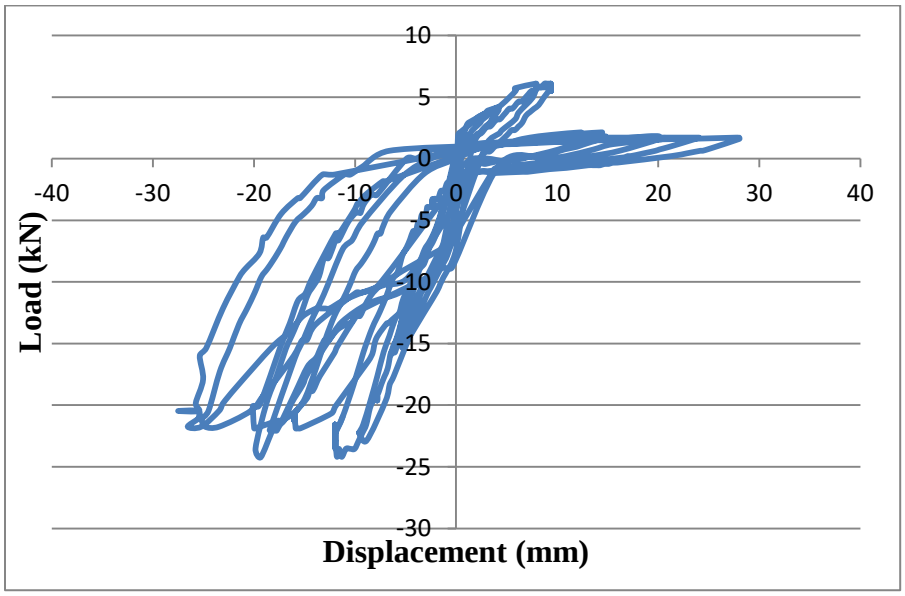

Figure 5.3 Load Vs Displacement Curve Retrofitted Complete Damaged (R1-CD)

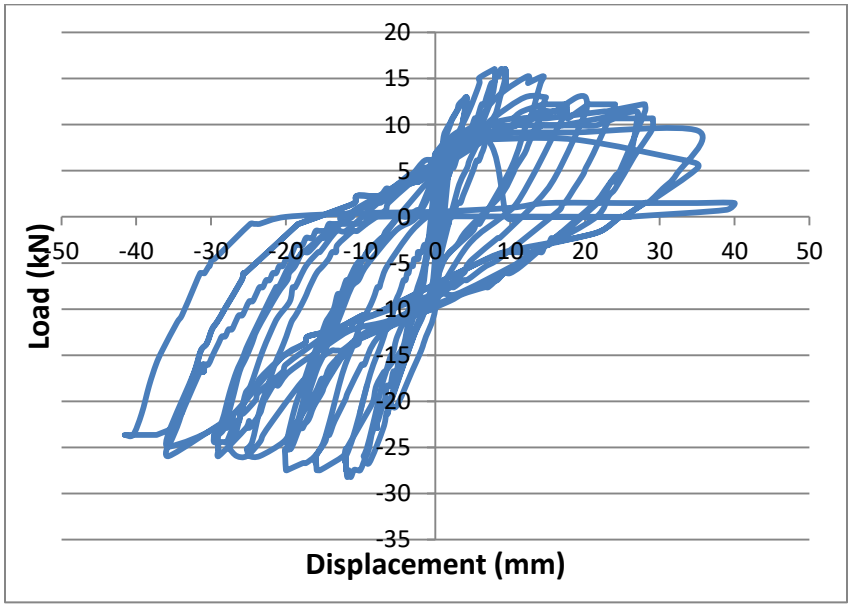

Figure 5.4 Load Vs Displacement Curve Retrofitted Complete Damaged (R2-MD)

5.3 INFLUENCE OF INITIAL DAMAGE LEVEL ON THE DUCTILITY OF RETROFITTED SPECIMENS

Load displacement envelop curve is used to calculate the ductility of controlled and retrofitted T-specimens shown in Figure 5.5. Load displacement curve revealed that pre peak behavior of R1-CD and R2-MD is almost similar, but considerable difference in post peak region. The load carrying capacity in post peak region degraded much quickly in R1-CD, whereas R-MD is stable in post peak region. Stability and improvement in post peak region attributes to improved ductility of the retrofitted specimens than C1-CD specimens. The ductility of R1-CD and R2-MD is 3.85 and 5 respectively refer Table 5.2. The comparison between the ductility of C1-CD and R1-CD revealed that the, R1-CD has 16% less and R2-MD has 16 % more ductility. The efficiency of ECC in post peak region is increased in R2-MD, it represents that the specimens initially damaged moderately performs well after retrofitting during cyclic loading.

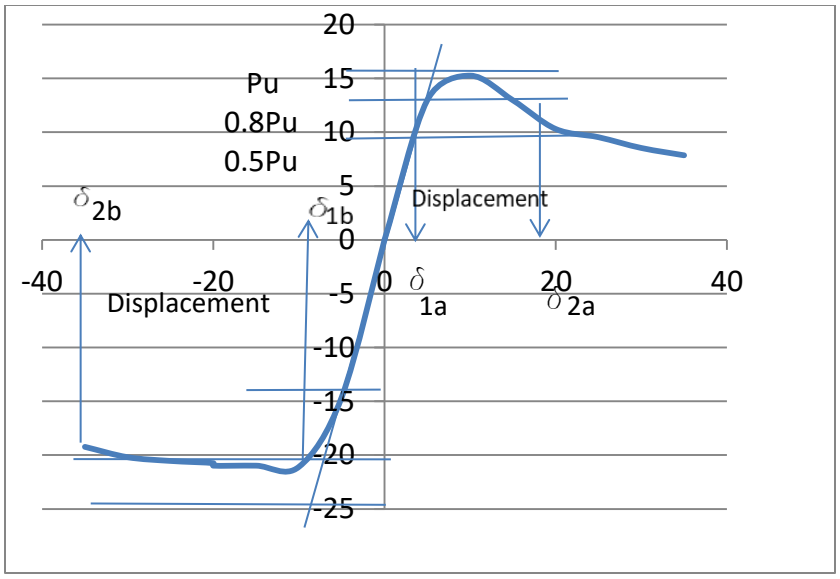

Figure 5.5 Procedures to Calculate Ductility of Beam Column Joint

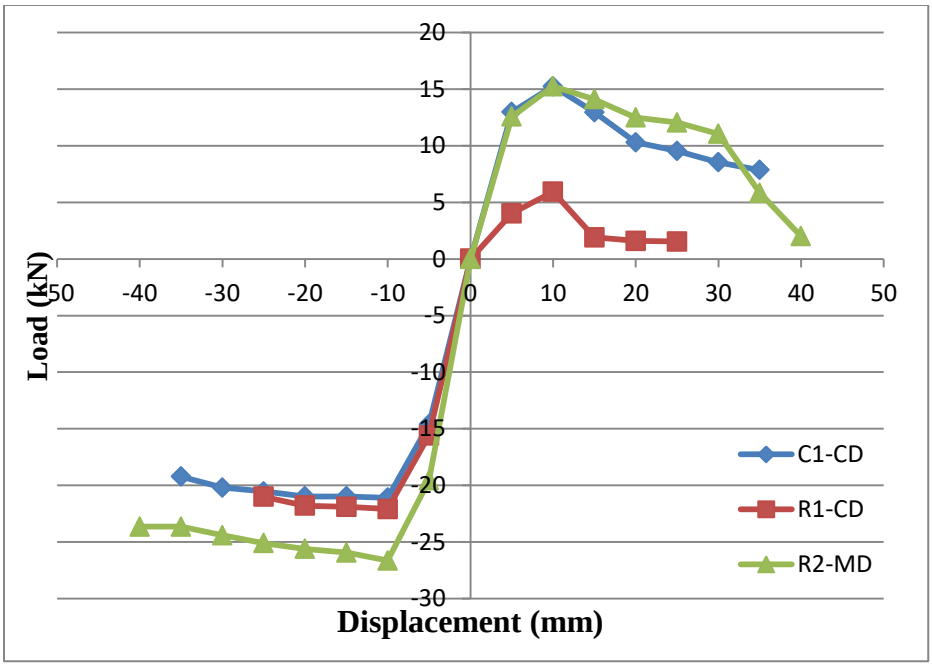

Figure 5.6 Load Displacement Envelop Curve of Beam Column Joint Specimen

Table 5.2 Displacement Ductility Calculation Controlled and Retrofitted Specimen

ID	Maximum positive load/Displacement (kN)	Maximum Negative Load/Displacement (kN)	Ultimate positive load (kN)	Ultimate negative load (kN)	Displacement (D)		Ductility (y) UD*/YD**
					Yield (D)	Ultimate (D)	
C1-CD	15.25/10mm	21.58/10mm	7.36/35mm	-20.22/30mm	10.5	48.5	4.6
R1-CD	5.94/5 mm	22.1/10mm	1.54/25mm	-21.01/25mm	10	38.5	3.85
R2-MD	15.25/10mm	-26.65/ 10mm	2.0025/40mm	-23.65/40mm	12	60	5

UD* Ultimate displacement

YD** Yield displacement

Displacement ductility = $\frac{\delta_{2a}+\delta_{2b}}{\delta_{1a}+\delta_{2a}}$ (see Figure 4.3)

5.4 STIFFNESS AND STRENGTH DEGRADATION

Stiffness is the slope of the line that joins peak positive cycle point to peak negative cycle point in a loading cycle (Villemure et al., 1995). The rigidity of controlled and revamped samples for each drift proportion is calculated. Load is the average of the peak load in positive and negative direction of the cycle and displacement is the value of load history in which cycle of load is applying in the specimens. In this experiment two cycles of same displacement is applying. Final stiffness is the average stiffness of two cycles. Drift is the ratio of the displacement of the specimen at initial position to the effective height.

From the drift vs stiffness curve shown in Figure 40 it is observed that R2-MD specimens has peak stiffness 18% higher than controlled C1-CD, but R1-CD has 28% lesser than controlled specimens. Increased average stiffness is found in the two moderately damaged R2-CD retrofitted specimens, but averaged stiffness found decreased in R1-CD in same drift ratio compare to C1-CD. No significant improvement in stiffness is found as drift goes higher for both R1-CD and R2-MD. In higher drift controlled and retrofitted specimens has not varyingly stiffness degradation is observed (See Figure 5.7). However R2-MD exhibits lower rater of stiffness degradation, since ECC is used in confinement zone of bean column joint.

Strength is defined as the ability of specimens to withstand against an applied cyclic load without failure. In each displacement level specimens resist the some value of load. This value of load is maximum in any of applied cycle which is considered as peak strength and from onwards of successive increased cycle's specimens lose to resist maximum peak load, this net retired capacity to resist load by joints in successive cycles is calculated in terms of strength degradation. Strength degradation is higher in lower drift ratio, but lower rate of degradation in higher drift ratio in positive lateral displacement (see Figure 5.8) in retrofitted specimens. Moderately damaged retrofitted specimens performed well as compare to controlled complete damaged specimens, but complete damaged retrofitted specimens perform satisfactory, since its strength degradation rate- is much higher as compare to C1-CD. In 4% drift ratio the strength degradation of R1-MD is 38% and C1-CD exhibits 44% degradation in same drift ratio. In 3% drift ratio R1-CD degrade strength by 73%, it is the highest degradation rate among all the specimens in 1.76% drift ratio. In R2-MD, rate of strength degradation is less among all specimens in drift ratio between 1%- 4%. During moderate earthquake no structural elements damage is permissible, structural members need to have adequate strength performed with in

elastic range so that no cracks formation. Therefore, lower rate of stiffness degradation in higher drift ratio improve the capacity of beam column joint in earthquake (Sasmal et al., 2011)

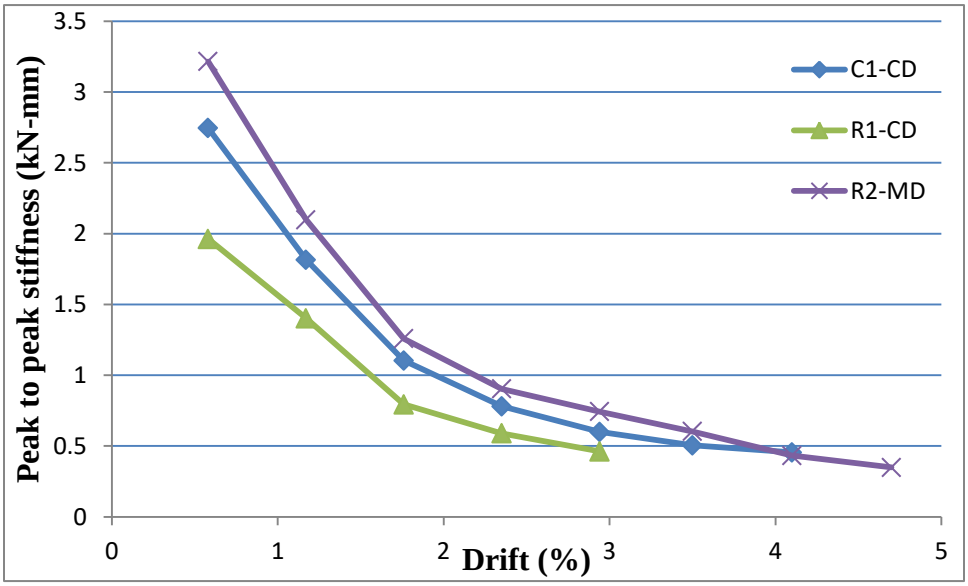

Figure 5.7 Stiffness Vs Drift Ratio of Controlled and Retrofitted Specimens

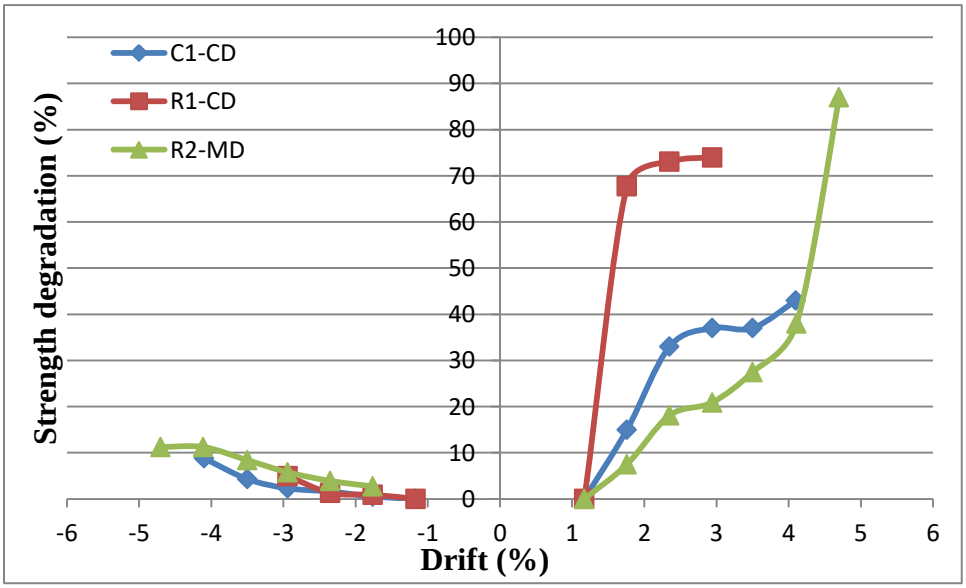

Figure 5.8 Strength Degradation Vs Drift Ratio

5.5 ENERGY DISSIPATION

It is the most significant parameter to measure earthquake response for ensuring the efficient structural response. Total Area within the boundary of hysteresis loop gives the total energy dissipation by the structure at different drift ratio. In terms of energy dissipation per cycle and cumulative energy dissipation, energy dissipation can be calculated. Cumulative energy

dissipation tells the total structural response for total duration of earthquake Figures 5.9 and 5.10 show the energy diffusion per cycle and the total energy diffusion of controlled and retrofitted joint beam column samples respectively. It is observed from the Figure 5.9 the energy dissipation per cycle is higher in retrofitted specimens as compare to controlled specimens under same reverse cyclic load. Total numbers of lateral load count in terms of cycle (ultimate displacement till 25mm) resisted by controlled R1-CD specimens is lower than C1-CD. The reason for limited ultimate displacement for R1-CD is its reinforcement were got yielded in prior complete damaged test. In contrast, initially moderately damaged (R2-MD) specimens has increased ultimate displacement which reaches up to 40 mm. The energy dissipation per cycle is increased for surely as a result of higher ultimate displacement of R2-MD. Higher energy dissipation property controls the crack propagation of retrofitted specimens.

Energy dissipation gives the response of the structure when structure is subjected in the earthquake for gross time period. Figure 5.10 controlled specimen (C1-CD) dissipated energy up to drift ratio 4.10%, whereas retrofitted specimen (R1-MD) dissipated energy up to 5.7 % drift ratio and energy dissipation is 1.05 times higher than C1-CD. R1-CD dissipated energy up to 2.94 % drift ratio which is 28% lesser then C1-CD, since pre yielding of reinforcement occurred in the specimen R1-CD. This result indicates that retrofitted specimens (R2-MD) have good energy dissipation capacity and better ductility. We found that energy dissipation capacity of retrofitted specimen of R2-MD is higher than C1-CD in every cycle, but R1-CD has comparatively poor performance in term of energy dissipation compare to C1-CD. Table 5.3 demonstrates the relative ability of all samples for energy dissipation.

Table 5.3 Comparison of Energy Dissipation Per Cycle Between Controlled Complete Damage And Retrofitted Beam Column Joint Specimens

Sr no	Cycle	ED of C1-CD	ED of R1-CD	% Improvement	ED of R1-MD	% Improvement
1	2	90.08	55.319	-38	97.42	8
2	4	303	190.6	-37	310.71	2
3	6	484.31	299.7	-38	563.82	16
4	8	969.47	342.4	-64	1011.7	4
5	10	1110	522.4	-52	1232.4	11
6	12	1220			1325.61	9

7	14	1350		1495.8	11

ED- Energy dissipation

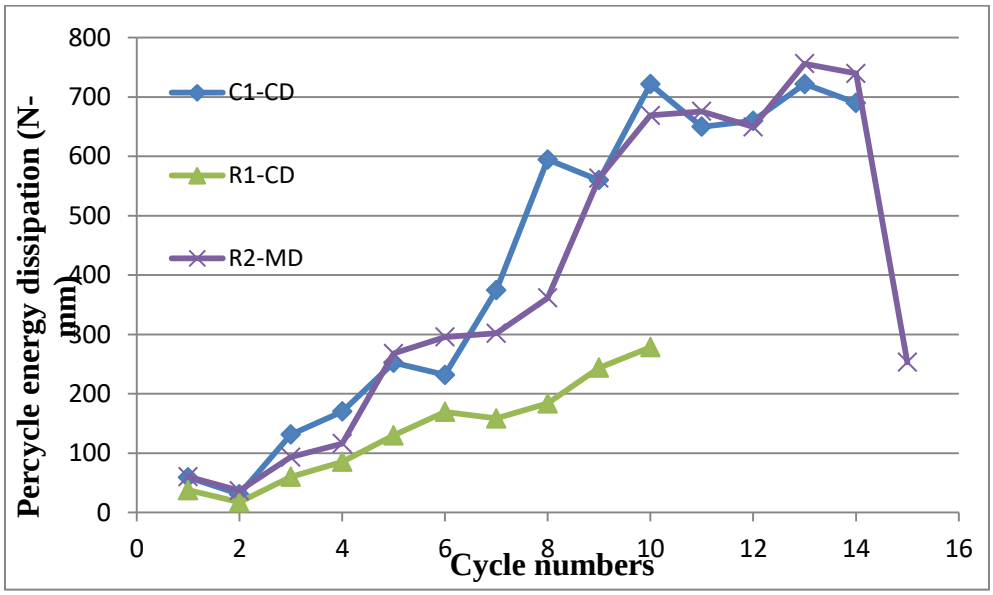

Figure 5.9 Energy Dissipation of Controlled and Retrofitted Specimen Per Cycle

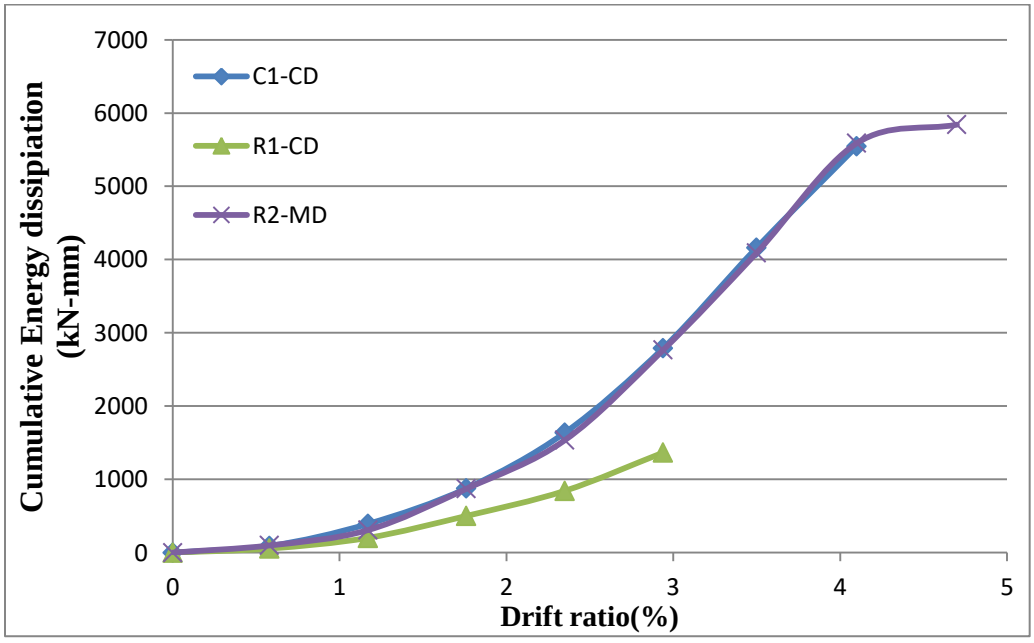

Figure 5.10 Cumulative Energy Dissipation Vs Drift Ratio

5.6 JOINT STRESS

During earthquake beam column joints is positioned to high horizontal shear stress (Murty et al., 2003). Horizontal shear stress in the joint are calculated using equation 8 and principal tensile stress or diagonal tensile stress induced in the joint is computed as equation 9.

$$\tau_{jh} = \frac{P}{A_{hcore}}\left(\frac{L_b}{d_b} - \frac{L_b + 0.5D_c}{L_c}\right) \quad (8)$$

$$\sigma_t = \frac{\sigma_p}{2} + \sqrt{\frac{{\sigma_p}^2}{4} + {\tau_{jh}}^2} \quad (9)$$

$$\sigma_p = \frac{(N_c + P)}{b_c h_c} \quad (10)$$

$\boldsymbol{\tau_{jh}}$ represents horizontal shear stress; P is the peak load applied in the end of beam in both negative and positive side. Lb is the longitudinal length and Lc is the column length. Dc and db, respectively, represent complete beam depth and efficient beam depth. A_{hcore} is the joint's cross-sectional region that participates in the horizontal shear force resistance. $\sigma_p$the compressive stress calculated by using equation 10. Nc is the 10% of the total axial load carrying capacity of the hydraulic jack column.

It is observed that retrofitted specimens R1-CD and R2-MD are sustaining higher diagonal tensile stress than controlled R1-CD in both positive and negative drift (see Figure 5.11). The ECC is best suited for moderately damaged specimens than completely specimens. Furthermore, ECC helps to resist high principle tensile stress for initially moderately damaged R-MD. We can conclude from this experiment that initial damage level of R1-CD slightly increase the principal tensile stress capacity in negative drift following with R2-MD and C1-CD, whereas in positive drift, stress capacity found increased in specimens R2-MD following by R1-CD and C1-CD

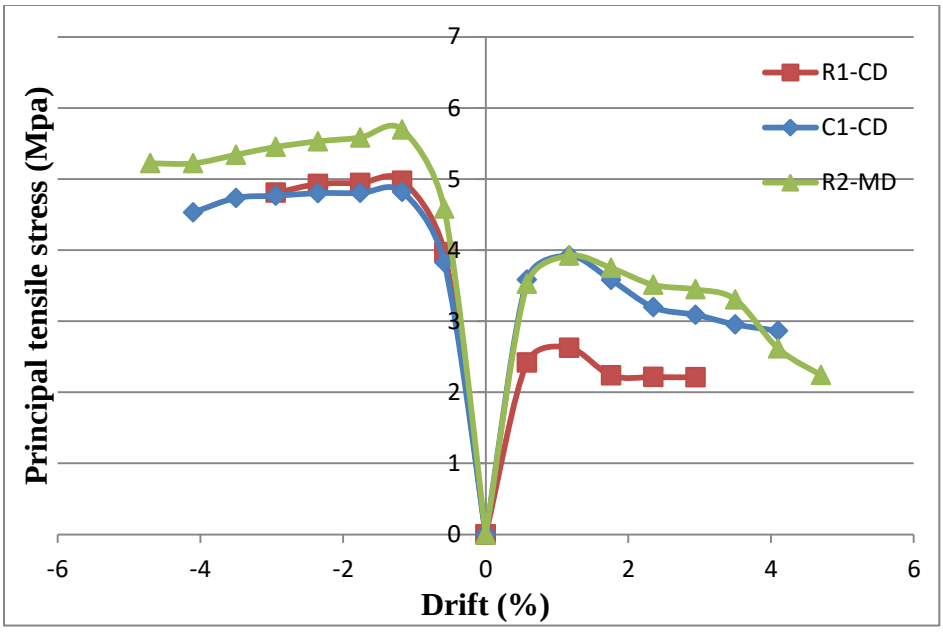

Figure 5.11 Principal Tensile Stress Vs Drift Ratio of Retrofitted and Control Specimen

5.7 CRACK AND FAILURE ANALYSIS

In C1-CD flexural crack starts to form in compression face in 5 mm displacement, Whereas tension reinforcement face experienced cracking at later displacement 10 mm and 15 mm. In both faces crack has generated due to yielding in the reinforcement. It is noticed that crack generated at compression face propagating towards joint zone in higher displacements, but no diagonal cracks has observed, since shear reinforcement provided throughout the column length. The reason behind this phenomenon is the principle tensile stress induced in ultimate displacement is less, hence no diagonal crack formation. The method of control of failure in C1-CD is the column face compression shown in Figure 5.12, since concrete start to spalling out in ultimate drift of 4.1% at compression face of beam. The close view of concrete spall out is cover in Figure 5.13. In specimen, R1-CD, initial crack start to appearing at 5 mm displacement in compression side. The cracks become more lucid in tension side as displacement cycles rises. In second cycle of 10mm displacement crack appears in face of beam column joint and it is continue to propagate and continue to widen up to final drift. In drift ratio of 2.9% shear reinforcement teared but no spalling out of concrete in the ultimate drift ratio in R1-CD and crack pattern is given in Figure 5.15. In the specimen C2-MD first crack appears in a 5mm displacement in compression face of the beam and crack start to appear in tension face at 10 mm and 15 mm displacement Figure 5.14 shows the crack pattern in joint specimen C2-MD.

The mode of failure in R1-CD and R2-MD are different from C1-CD. The failure mode in the C1-CD is compression face, but all the retrofitted specimens including R1-CD do not govern failure in compression. In R1-CD and R2-MD rotation takes place at the face of beam column joint and through this rotation energy is dissipated throughout successive load history till the ultimate drift ratio. By effect of this process cracks are getting widen up in the joint face area. This failure mode, failure at joint face is the evidence of strong column and weak beam mechanism. PVA fiber present in the ECC helps to bridge the small crack formed in the joints and beam region, where as steel fibers present in the ECC helps to bridge the crack formed in joint face of the beam column in higher drift ratio. No diagonal crack been formed in both controlled and retrofitted specimens during the experiment, since shear reinforcement is provided in column in joint region and ECC additionally helps to make joint more confined, which increases the tensile strength of joint. Total flexural strength capacity is utilized in retrofitted specimens. From Figure 5.15 and 5.16 it is closely observed that plastic hinge is formed, which represents considerable plastic deformation in beam is allowed and resist the shear deterioration in beam column joint area. Hence, ECC performed optimum as retrofitting material for non-seismic designed structural element.

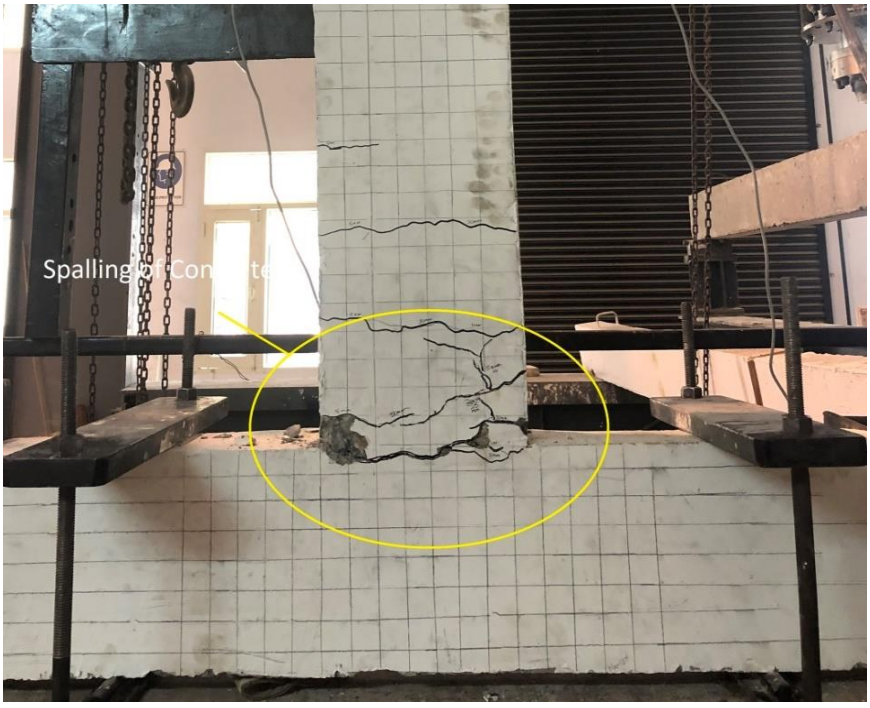

Figure 5.12 Flexural Crack Pattern of Specimen C1-CD

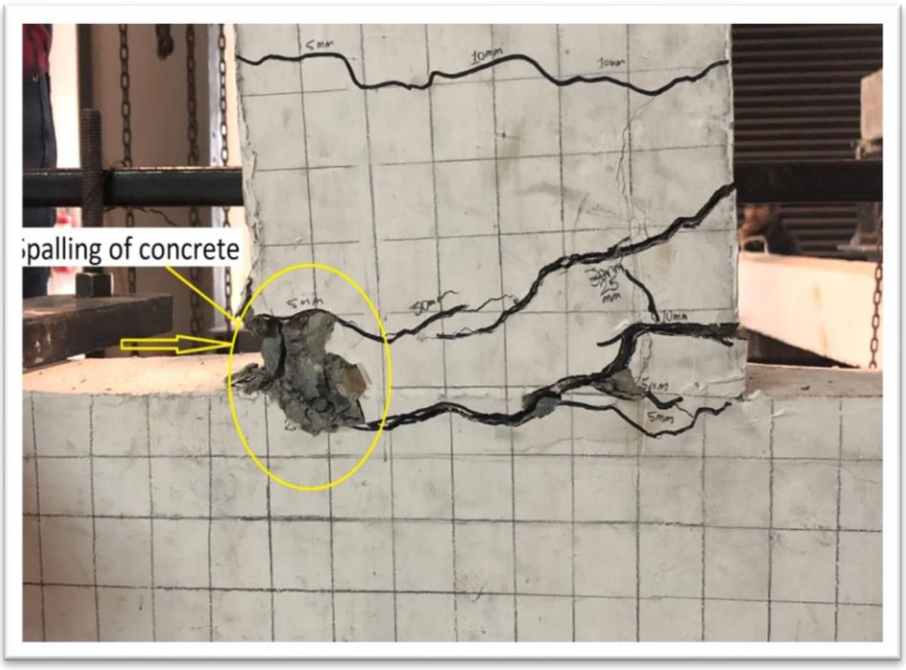

Figure 5.13 Compression Face Failure of Specimen C1-CD at 35 mm Ultimate Lateral Displacement

Figure 5.14 Crack Pattern in Specimen C2-MD

Figure 5.15 Ultimate Displacement Failure of Specimen R1-CD at 40 mm

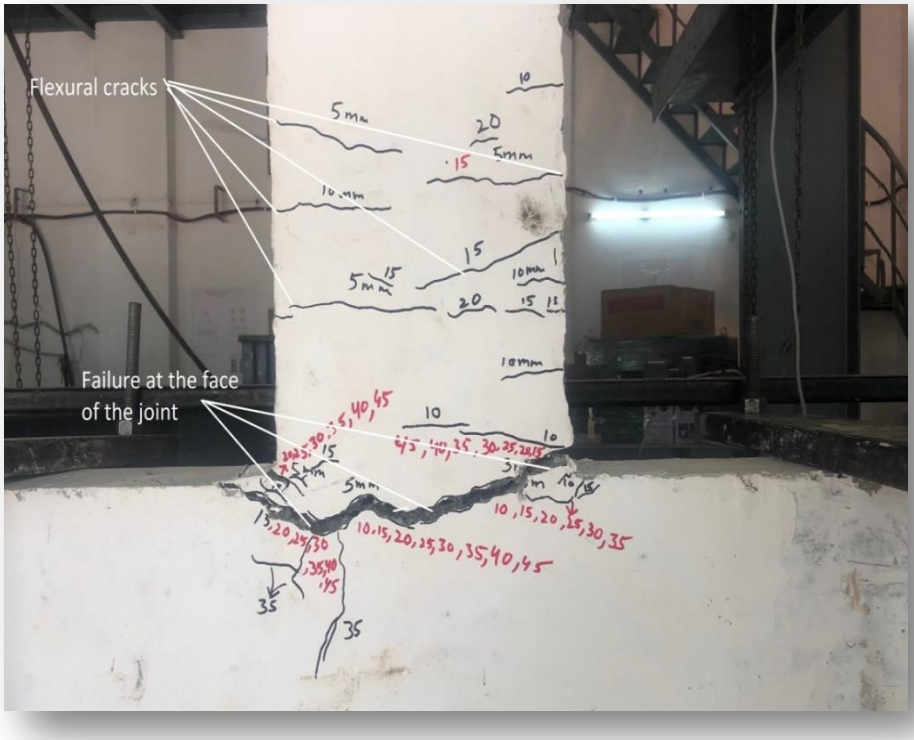

Figure 5.16 Failure of Specimens R2-MD at Ultimate Displacement of 40 mm

CHAPTER 6

CONCLUSION

The result obtained in this experimental study of controlled and retrofitting beam column joint has shown important result about the feasibility of ECC as a retrofitting material in structural element subjected to earthquake load. The following conclusion can draw from the experimental study.

1. Retrofitting specimens showed important improvement over the controlled samples in the pre- and post-yield regions. The ductility of R2-MD is increased by 8 % as compare to controlled C1-CD, but R2-CD the ductility decreased ductility by 16 % than C1-CD. It clearly shows that initial damage level has significant influence in ductile performance of ECC as a retrofitting material.
2. Peak to peak stiffness found higher in the retrofitted specimens (R2-MD) than R1-CD and controlled specimen C1-CD. R2-MD performed well in lower and higher drift ratio compare to C1-CD. R2-MD success to retain stiffness in higher drift ratio of 4.7% among rest specimens including R1-CD.
3. Strength degradation is higher in R1-CD. It is 67% in positive drift of 1.76%, since it was got failed in compression in initial complete damage testing. Higher magnitude of strength degradation is therefore discovered in positive drift. In positive ultimate drift ratio of 4.1 %, R2-MD able to retain strength only 38% strength degradation in maximum positive drift and 11.5 % strength degradation in ultimate negative drift. It is the lowest strength degradation compared to both C1-CD and R1-CD.
4. Energy dissipation capacity of BCJ is considerably influenced by initial damage level. In lower drift ratio, controlled and retrofitted specimen dissipated almost equal energy, but in the higher drift ratio R1-CD down performed as compare to R2-MD and C1-CD. The R1-CD dissipated 1365 kN-mm at 2.94% drift ratio. The R2-MD dissipated 5841 kN-mm at 4.7% ultimate drift ratio. This value indicates that initially moderate damaged retrofitted specimen dissipated higher energy then initially completely damaged specimens. Higher magnitude of force degradation is thus discovered in favorable drift.
5. Joint principal stress capacity is increases substantially in retrofitted specimens compared to controlled specimens. In positive drift, principal tensile stress capacity is effected as initial damage level increased from slight to completely such as R1-CD has relatively less

stress capacity maximum of 2.6 MPa, whereas R2-MD has 3.91 MPa. However stress capacity increased is in upper side than control specimens. In R2-MD, principal tensile stress capacity is higher in ultimate drift compare to R1-CD and C1-CD. Stress capacity is found less in positive drift compare to negative drift in both controlled and retrofitted specimens.

REFRENCES

1. Bajaj, K., Shrivastava, Y., & Dhoke, P. (2013). Experimental study of functionally graded beam with fly ash. *Journal of The Institution of Engineers (India): Series A*, *94*(4), 219-227.
2. Banjara, N. K., Ramanjaneyulu, K., Sasmal, S., & Srinivas, V. (2016). Flexural fatigue performance of plain and fibre reinforced concrete. *Transactions of the Indian Institute of Metals*, *69*(2), 373-377.
3. Chen, S., He, R., Li, Y., Xing, M., & Cong, P. (2013). Influence of thickeners on cement paste structure and performance of engineered cementitious composites. *Journal of Wuhan University of Technology-Mater. Sci. Ed.*, *28*(2), 285-290.
4. Chidambaram, R. S., & Agarwal, P. (2015). Performance evaluation of geogrid-confined beam-column joints with steel fiber reinforced concrete under cyclic loading. Journal of Testing and Evaluation, 44(1), 582-598.
5. Chidambaram, R. S., & Agarwal, P. (2015). Seismic behavior of hybrid fiber reinforced cementitious composite beam–column joints. Materials & Design, 86, 771-781.
6. Choi, J. I., Jang, S. Y., Kwon, S. J., & Lee, B. Y. (2017). Tensile behavior and cracking pattern of an ultra-high performance mortar reinforced by polyethylene fiber. *Advances in Materials Science and Engineering*, *2017*.
7. Hossain, K. M. A. (2004). Properties of volcanic pumice based cement and lightweight concrete. *Cement and concrete research*, *34*(2), 283-291.
8. Huang, X., Ranade, R., & Li, V. C. (2012). Feasibility study of developing green ECC using iron ore tailings powder as cement replacement. *Journal of Materials in Civil Engineering*, *25*(7), 923-931.
9. Ilia, E., & Mostofinejad, D. (2019). Seismic retrofit of reinforced concrete strong beam–weak column joints using EBROG method combined with CFRP anchorage system. *Engineering Structures*, *194*, 300-319.
10. Kabir, S. M., Alengaram, U. J., Jumaat, M. Z., Sharmin, A., & Islam, A. (2015). Influence of molarity and chemical composition on the development of compressive strength in POFA based geopolymer mortar. *Advances in Materials Science and Engineering*, *2015*.

11. Kaliluthin, A. K., & Kothandaraman, S. (2017). Performance Evaluation of Exterior Beam–Column Joint with Core Reinforcement Technique Subjected to Reverse Cyclic Loading. *Arabian Journal for Science and Engineering*, *42*(9), 3673-3687.
12. Kalra, M., Kumar, M., & Singh, N. B. (2019). Performance evaluation of Concrete made from Fly Ash blended cement in the presence of Silicone Hydrophobic Powder-50 and Silica Fume. *Materials Today: Proceedings*, *15*, 677-686.
13. Kang, S. T., Lee, K. S., Choi, J. I., Lee, Y., Felekoğlu, B., & Lee, B. Y. (2016). Control of tensile behavior of ultra-high performance concrete through artificial flaws and fiber hybridization. *International Journal of Concrete Structures and Materials*, *10*(3), 33-41.
14. Kim, J. K., Kim, J. S., Ha, G. J., & Kim, Y. Y. (2007). Tensile and fiber dispersion performance of ECC (engineered cementitious composites) produced with ground granulated blast furnace slag. *Cement and Concrete Research*, *37*(7), 1096-1105.
15. Li, V. C. (2009). Damage Tolerant ECC for Integrity of Structures Under Extreme Loads. In *Structures Congress 2009: Don't Mess with Structural Engineers: Expanding Our Role* (pp. 1-10).
16. Li, V. C., & Yang, E. H. (2007). Self healing in concrete materials. In *Self healing materials* (pp. 161-193). Springer, Dordrecht.
17. Ma, C. K., Apandi, N. M., Sofrie, C. S. Y., Ng, J. H., Lo, W. H., Awang, A. Z., & Omar, W. (2017). Repair and rehabilitation of concrete structures using confinement: A review. *Construction and Building Materials*, *133*, 502-515.
18. Marar, K., Eren, Ö., & Roughani, H. (2017). The influence of amount and aspect ratio of fibers on shear behaviour of steel fiber reinforced concrete. *KSCE Journal of Civil Engineering*, *21*(4), 1393-1399.
19. Ndiaye, D., Matuana, L. M., Morlat-Therias, S., Vidal, L., Tidjani, A., & Gardette, J. L. (2011). Thermal and mechanical properties of polypropylene/wood-flour composites. *Journal of applied polymer science*, *119*(6), 3321-3328.
20. Nematollahi, B., Qiu, J., Yang, E. H., & Sanjayan, J. (2017). Micromechanics constitutive modelling and optimization of strain hardening geopolymer composite. *Ceramics International*, *43*(8), 5999-6007.
21. Nethercot, D. A. (2001). The Paramount Role of Joints into the Reliable Response of Structures-CC Baniotopoulos and F. Wald (Eds); NATO Science Series published by Kluwer Academic Publishers, Dordrechtand, December 2000, pp. 451, Price@ $116, ISBN 0-7923-6700-6. *Engineering Structures*, *10*(23), 1364.

22. Özbay, E., Šahmaran, M., Lachemi, M., & Yücel, H. E. (2013). Self-Healing of Microcracks in High-Volume Fly-Ash-Incorporated Engineered Cementitious Composites. *ACI Materials Journal*, *110*(1).
23. Pan, Z., Wu, C., Liu, J., Wang, W., & Liu, J. (2015). Study on mechanical properties of cost-effective polyvinyl alcohol engineered cementitious composites (PVA-ECC). *Construction and Building Materials*, *78*, 397-404.
24. Parvin, A., & Granata, P. (2000). Investigation on the effects of fiber composites at concrete joints. *Composites Part B: Engineering*, *31*(6-7), 499-509.
25. Qian, S., Zhou, J., De Rooij, M. R., Schlangen, E., Ye, G., & Van Breugel, K. (2009). Self-healing behavior of strain hardening cementitious composites incorporating local waste materials. *Cement and Concrete Composites*, *31*(9), 613-621.
26. Ramezanianpour, A. A. (2014). Cement replacement materials. *Springer, Berlin. doi*, *10*, 978-3.
27. Saathappan, V. R. A., Raghunath, P. N., & Suguna, K. (2011). Adaptive neuro-fuzzy model for performance evaluation of RC T-beams with externally bonded GFRP reinforcement. *Journal of Reinforced Plastics and Composites*, *30*(24), 2015-2023.
28. Şahmaran, M., Lachemi, M., Hossain, K. M., & Li, V. C. (2009). Internal curing of engineered cementitious composites for prevention of early age autogenous shrinkage cracking. *Cement and concrete research*, *39*(10), 893-901.
29. Sahmaran, M., Yildirim, G., & Erdem, T. K. (2013). Self-healing capability of cementitious composites incorporating different supplementary cementitious materials. *Cement and Concrete Composites*, *35*(1), 89-101.
30. Said, S. H., & Razak, H. A. (2016). Structural behavior of RC engineered cementitious composite (ECC) exterior beam–column joints under reversed cyclic loading. *Construction and Building Materials*, *107*, 226-234.
31. Sasmal, S., Ramanjaneyulu, K., Novák, B., Srinivas, V., Kumar, K. S., Korkowski, C., ... & Iyer, N. R. (2011). Seismic retrofitting of nonductile beam-column sub-assemblage using FRP wrapping and steel plate jacketing. *Construction and Building Materials*, *25*(1), 175-182.
32. Shafaei, J., Hosseini, A., & Marefat, M. S. (2014). Seismic retrofit of external RC beam–column joints by joint enlargement using prestressed steel angles. *Engineering Structures*, *81*, 265-288.

33. Sharma, R., & Bansal, P. P. (2019). Behavior of RC exterior beam column joint retrofitted using UHP-HFRC. Construction and Building Materials, 195, 376-389.
34. Sundarraja, M. C., & Rajamohan, S. (2008). Flexural strengthening effect on RC beams by bonded composite fabrics. *Journal of reinforced Plastics and Composites*, *27*(14), 1497-1513.
35. Swamy, R. N., & Jojagha, A. H. (1982). Impact resistance of steel fibre reinforced lightweight concrete. *International Journal of Cement Composites and Lightweight Concrete*, *4*(4), 209-220.
36. Thai, H. T., & Kim, S. E. (2009). Practical advanced analysis software for nonlinear inelastic analysis of space steel structures. *Advances in engineering software*, *40*(9), 786-797.
37. Torabi, A., & Maheri, M. R. (2017). Seismic repair and retrofit of RC beam–column joints using stiffened steel plates. *Iranian Journal of Science and Technology, Transactions of Civil Engineering*, *41*(1), 13-26.
38. Wang, G. L., Dai, J. G., & Bai, Y. L. (2019). Seismic retrofit of exterior RC beam-column joints with bonded CFRP reinforcement: An experimental study. *Composite Structures*, *224*, 111018.
39. Wu, M., Johannesson, B., & Geiker, M. (2012). A review: Self-healing in cementitious materials and engineered cementitious composite as a self-healing material. *Construction and Building Materials*, *28*(1), 571-583.
40. Yang, Y., Sneed, L. H., Morgan, A., Saiidi, M. S., & Belarbi, A. (2015). Repair of RC bridge columns with interlocking spirals and fractured longitudinal bars–An experimental study. *Construction and Building Materials*, *78*, 405-420.
41. Yuan, F., Pan, J., Xu, Z., & Leung, C. K. Y. (2013). A comparison of engineered cementitious composites versus normal concrete in beam-column joints under reversed cyclic loading. *Materials and structures*, *46*(1-2), 145-159.
42. Yuksel, E., Karadogan, H. F., Bal, İ. E., Ilki, A., Bal, A., & Inci, P. (2015). Seismic behavior of two exterior beam–column connections made of normal-strength concrete developed for precast construction. *Engineering structures*, *99*, 157-172.
43. Zhang, J., Gong, C., Guo, Z., & Ju, X. (2009). Mechanical performance of low shrinkage engineered cementitious composite in tension and compression. *Journal of composite materials*, *43*(22), 2571-2585.

44. Zhang, R., Matsumoto, K., Hirata, T., Ishizeki, Y., & Niwa, J. (2015). Application of PP-ECC in beam–column joint connections of rigid-framed railway bridges to reduce transverse reinforcements. *Engineering Structures*, *86*, 146-156.

45. Zhou, J., Qian, S., Beltran, M. G. S., Ye, G., van Breugel, K., & Li, V. C. (2010). Development of engineered cementitious composites with limestone powder and blast furnace slag. *Materials and Structures*, *43*(6), 803-814.